JNC TJ7400 2000-012

SKB TRUE Block Scale 試験における解析作業の実施

（核燃料サイクル開発機構 契約業務報告書）

2000年3月

三菱商事株式会社

JNC TJ7400 2000-012
2000年3月

SKB TRUE Block Scale試験における解析作業の実施

吉添 誠*　William Dershowitz**

要旨

本報告書は、Golder社により平成11年度（1999年-2000年）に実施されたエスポ TRUE ブロック試験に関わる核燃料サイクル機構（JNC）殿への支援を取り纏めるものである。平成11年度の主要な業務は以下の通りである。

- 適切な構造モデルの構築
- 亀裂ネットワーク中の亀裂交差ゾーン（FIZ）が溶質の移行に及ぼす影響の評価
- トレーサー試験及び試験設計の支援
- 水理及びトレーサー試験結果の解釈
- 周辺微小割れ目の統計解析
- PAWorksチャネルネットワークモデルの構築
- チャネルネットワークモデルの調整
- 事前試験及びフェーズ A トレーサー試験の予備的チャネルネットワーク解析

Golder 社の平成 11 年度の JNC 殿への支援に関わる技術的情報は、本報告書において参照されている詳細なプロジェクト報告書に記載されている。

本報告書は、三菱商事（株）が核燃料サイクル開発機構の委託により実施した業務に関するものである。
機構担当部課室：東濃地科学センター 地層科学研究グループ　竹内 真司
*　三菱商事株式会社 石炭・原子燃料事業部
**　Golder Associates Inc., Seattle, USA

ABSTRACT

This report describes Äspö TRUE-Block experiment support provided to JNC by Golder Associates Inc. during the Heisei-11 (1999-2000) fiscal year. Major efforts during HY-11 included:

- derivation of an appropriate structural model
- evaluation of fracture intersection zone (FIZ) effects on solute transport in fracture networks
- support to tracer test and experimental design
- interpretation of hydraulic and tracer test results
- evaluation of background fracture statistics
- implementation of PAWorks channel network models
- channel network model calibration
- predictive channel network simulations of pre-tests and Phase A tracer tests.

Technical information about Golder Associates HY-11 support to JNC is provided in detailed project reports referenced in this annual report.

概要

核燃料サイクル機構（JNC）殿は、エスポ・スウェーデン硬岩研究所（HRL）における国際エスポ TRUE ブロックスケール試験に、フルパートナーとして参加されている。この試験は、50 ないし 100m スケールにおける低透水性亀裂ネットワークでの地下水流動および物質移行に関する理解を深めるためのものである。

1999 年、Golder 社は、以下を含む本計画の主要部分のほぼ全てに参加された JNC 殿を支援した。

- 水理データ、トレーサーの移行および亀裂データの解析
- 亀裂交差ゾーン（FIZ）の理論的研究
- 試験設計
- チャネルネットワークのモデル化およびこれに基づく試験
- チャネルネットワーク内の地下水流動および物質移行のシミュレーション

割れ目データの解析

1999 年、Golder 社は周辺微小割れ目の解析を実施した。この解析は、1997 年から実施されている TRUE ブロックスケール試験のための亀裂ネットワーク（DFN）およびそれに関連するチャネル・ネットワーク（CN）の各モデルを開発するためのものである（例えば、Dershowitz and Uchida, 1999 参照）。この研究の目的は、試錐孔が亀裂#13、#20、#21 および#22 と交差する領域の周辺において周辺微小割れ目をモデリングするための定量的基礎を得ることである。この“TTS（Tracer Test Stage）領域”およびその中の亀裂は、TRUE ブロックスケール試験のトレーサー試験段階（TTS）における焦点である（図 1）。

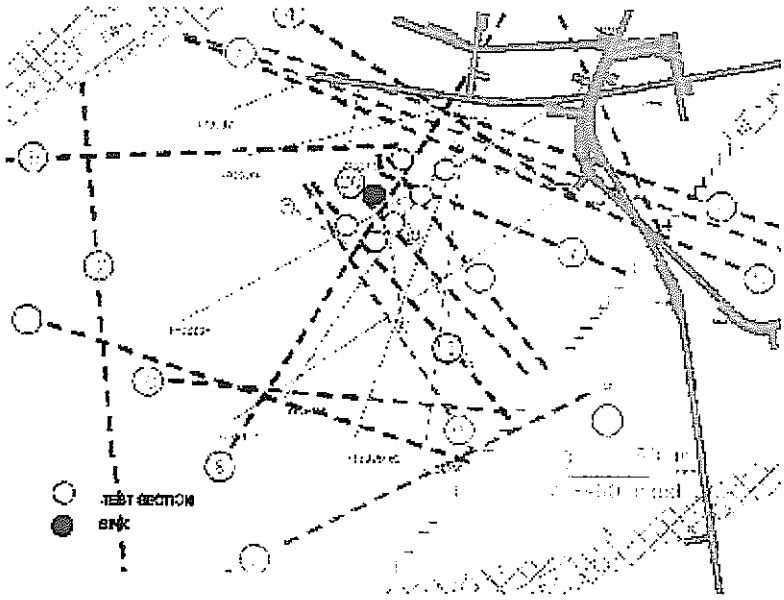

図 1：トレーサー試験領域

1999 年、GOLDER 社は、空間的割れ目構造、オリエンテーション、割れ目強度、および透水量係数の解析を行った。これらの解析は Posiva 流動検層中で同定された変化点に基づくものである。これらの変化点を図２に示す。図３および図４は、GOLDER 社が TTS 領域 Posiva 流動検層の変化点データに対して実施した透水量係数および割れ目の空間構造に関する各解析の一例を示すものである。

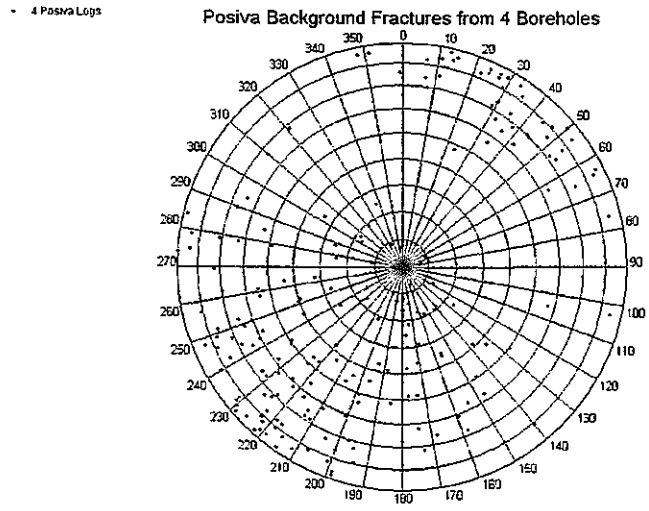

図２：TTS 試錐孔に基づく Posiva 流動検層から得られた割れ目

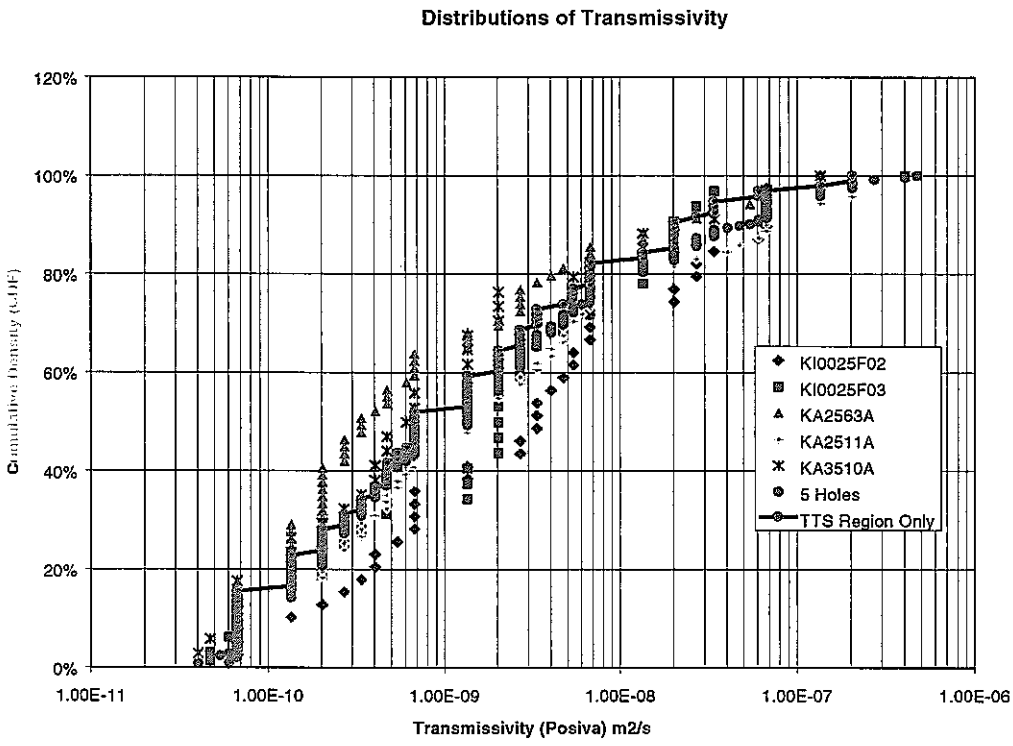

図３：Posiva 流動検層による割れ目の透水量係数分布

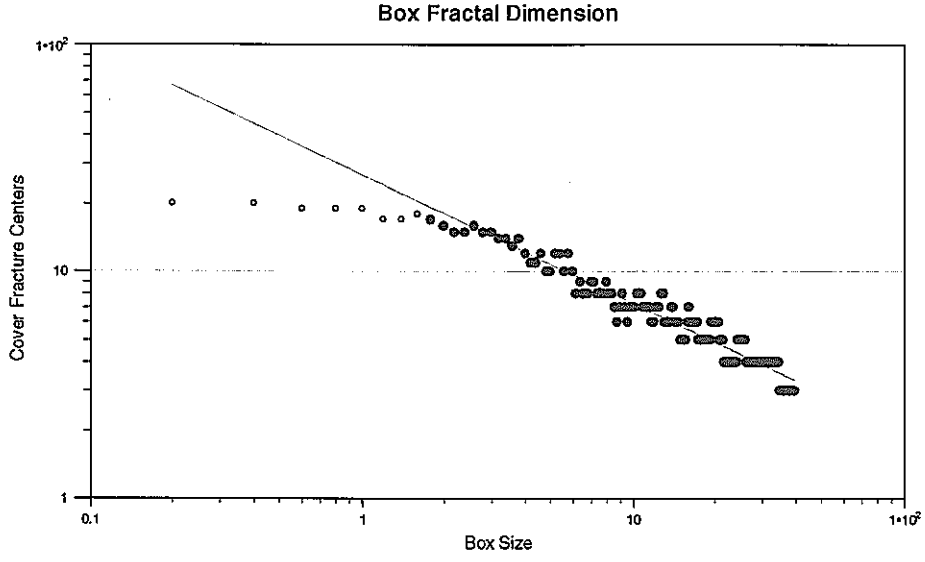

図４：周辺微小割れ目の空間解析例

割れ目交差ゾーンの理論的考察

1999年、GOLDER社は、トレーサー試験設計の実施可能性を調査するべく、広範囲にわたるシミュレーションによる理論的考察を行った。かかるトレーサー試験とは、TRUEブロックスケール対象領域中でのトレーサー試験による割れ目交差ゾーン（FIZ）効果を数量化するために使用し得るものである。目的達成のために、一連のシミュレーションによるトレーサー試験が一般的な幾何学的割れ目構造に対して実施され、割れ目交差部分における高い透水量係数によってFIZ効果が定義された。この一般的考察に続き、詳細なサイト特性調査プログラムで同定された亀裂#20、#21および#22の幾何学的構造および特性に基づき、更なる考察が行われた。

干渉試験中におけるトレーサー移行に対するFIZ効果を事前解析する概念モデルを図5に示す。割れ目交差ゾーンは移行経路上において、次の各効果をもたらし得る。(a)より高い透水性、(b)より低い透水性（流動障害）、(c)より高い間隙率（より低い速度）、(d)より高いまたはより低い反応表面積（より多いまたはより少ない収着と拡散）。表1にFIZ事前解析の検討結果を示す。

表1：FIZ検討結果の例

	Median Breakthrough Time t_{50}, (h)			
Source interval	KI2563	KI0023	KI0025F02	KI0025
Sink interval	New_1	new_1	new_1	new_2
Case 1: Homogeneous	80.52	52.36	27.77	27.01
Case 2: Homogeneous with increased T for FIZ ($1e^{-4}$ m/s)	161.51	94.29	27.14	59.28
Case 3: Heterogeneous	346.73	187.82	61.91	51.02
Case 4: Heterogeneous with increased T for FIZ ($1e^{-5}$ m/s).	375.73	185.01	58.26	46.15
Case 5: Heterogeneous with increased T for FIZ ($1e^{-4}$ m/s).	445.97	165.95	94.77	112.97
Case 6: Heterogeneous with increased T for FIZ ($1e^{-2}$ m/s).	834.73	564.26	87.28	642.19

1999年のGOLDER社による考察では、考察対象となったほぼ全てのケースにおいて、FIZ効果の同定はその存在が明らかであるにもかかわらず非常に困難であることが結論付けられた。しかしFIZの間隙率がより大きい場合には、FIZを含む経路上でのより低い速度の同定が可能となるであろう。このことは主に非吸着性トレーサーの場合に明らかとなるであろう。吸着性トレーサーの場合には、FIZの反応表面積が移行経路上のそれよりも著しく小さければ、FIZ効果は目で見える形で確認できるであろう。

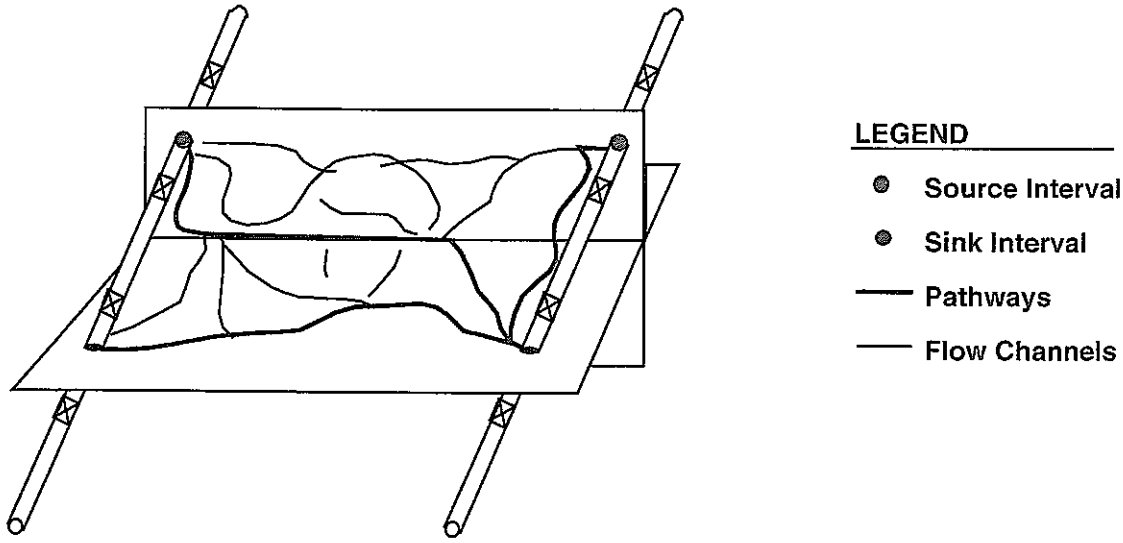

図５：割れ目交差ゾーン

概念モデルの開発

GOLDER 社は、トレーサー試験段階（TTS）の焦点となる領域の適切な水理構造モデルの開発において、TRUE ブロックスケール試験チームを援助した。その際には水理学的データセットの解析がなされ、かかるデータセットには、5-m パッカー流動検層（KI0023B、KI0025F）、Posiva 流動検層（KI0025F02、KA2563A）、圧力上昇試験（KI0023B、KI0025F02）、圧力干渉試験、掘削応答、ならびにトレーサー希釈試験が含まれていた。JNC は、最初の三つのトレーサー予備試験における圧力干渉および希釈の各試験の結果を特に強調している。三つの予備試験では、ソースとして、構造 13（KI0023B-3）、構造 21（KI0023B-5）および構造 20（KI0025F02-5）が使用された。

トレーサー試験は、番号付けされた二つの亀裂構造すなわち構造 20 および 13 の周辺領域において行われるように設計されている。圧力応答を解析するための主要ツールは、水位低下と距離とをプロットしたものを観測地点－揚水点間の距離の二乗で割ったものである。これらの点が標準曲線上に並ぶ程度または集まる傾向により、システムの均質性または複数の透水性の存在が示される。これらのプロットは、各揚水試験の水位低下のプロットにより完成される。図 6 に TRUE ブロックスケール対象領域において解析された試錐孔を示す。

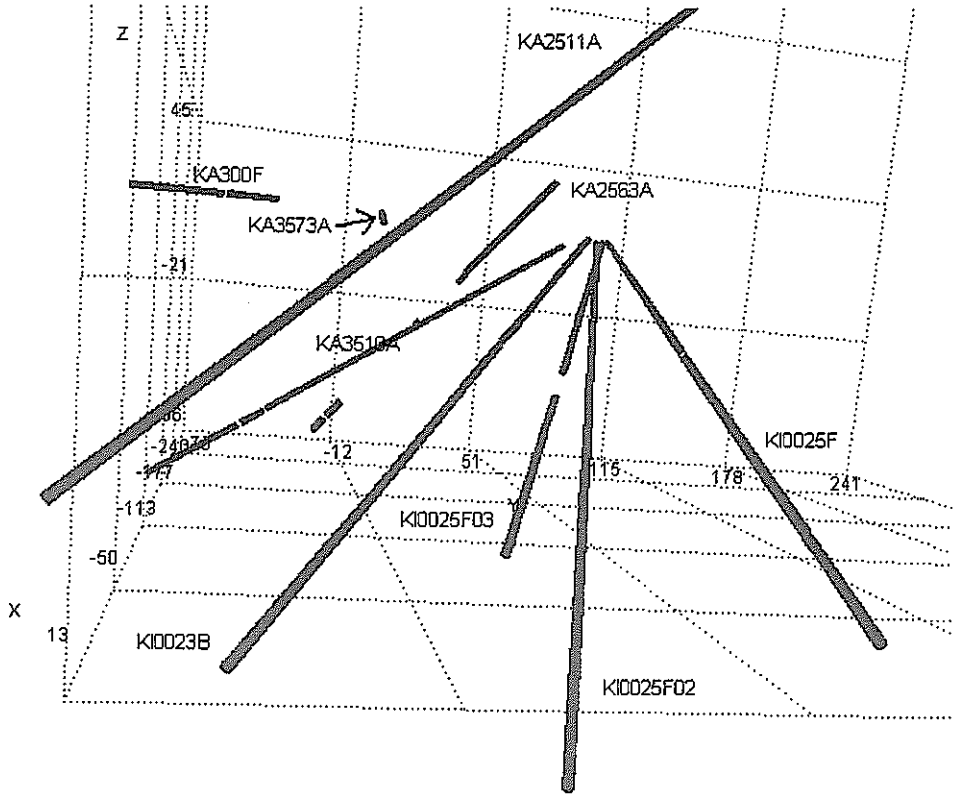

図 6：PT-3 予備試験での距離－水位低下の関係

総合的な考察の結果は、'99 年 3 月の構造モデルによる TRUE ブロックの主要な水みちの存在が大部分において説明可能であることを示している。各特徴の簡単な説明は以下の通りである。水理学的データおよび割れ目構造の連続性の様子を図 7 に示す。この図では、データ・プロットの便宜上、試錐孔を並行なものとして表している。長さ軸は、構造 20 の位置が“0”に来るように調節されている。この調節により試錐孔は整列され、異なる試錐に共通する特徴についての視覚による比較が可能となっている。

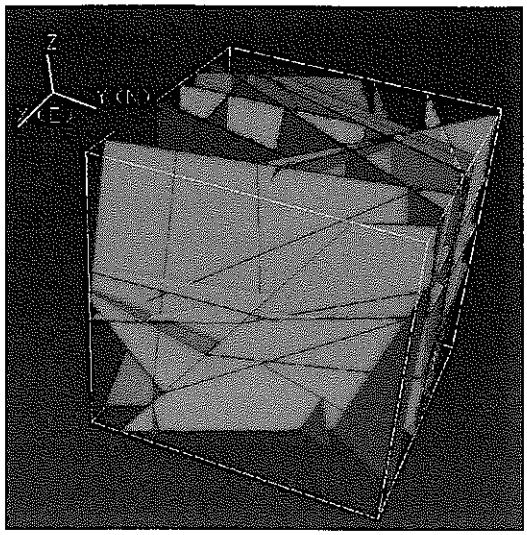

• 27 Fractures, colored by transmissivity

• External boundary is 500m x 500m x 500m

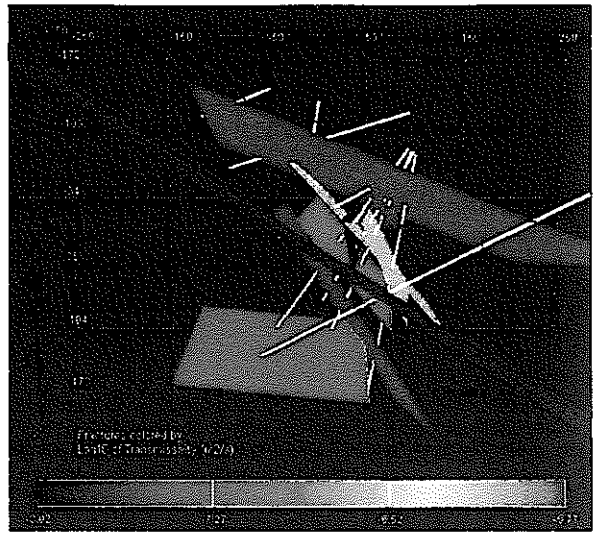

• 9 fractures modified in October 1999 structural reconciliation report

図 7：TRUE ブロックスケール構造モデル

フローメータ検層の変化点および圧力上昇データは、各ゾーンからの推定定常流動に比例する高さのバーにより示される。5-m 流動検層のデータはバー・チャートで示され、掘削時の顕著な流入または圧力応答の位置は各試錐孔を示す線の下の三角形によって示される。チャート上の水平な各線は試錐孔を表す。四角形はパッカー位置を示し、太線は観測区間を示す。'99 年 3 月の構造モデルは黄色で示され、最近のデータから推定される水みちは透明な灰色網掛けで示される。

構造 20 はブロックの中心部に位置する主要な水みちであり、試錐孔配列の約 80m 上にある KA2511A を除く全ての試錐孔に現れている。現行の予備試験により構造 20 の位置とその透水性が確認されている。

構造 13 と構造 20 は異なる亀裂であり、連結している。構造 13 における圧力応答から、KI0023B および KA2563A の各試錐孔間の強い連結が示される。KI0025F02 ではより圧力応答が遅くまた水位低下も低く、連結が弱くなっている。構造 13 は、KI0025F 間では水理学的にほぼ消失していると思われる。

KI0025F02-3 と交差が想定される構造の亀裂位置は、むしろ構造 20 とより強い連結が認められる。このことは PT-2 および PT-3 の各試験で観測されたより大きな水位低下が示す通りである。この亀裂は KI0025F-3 へ連続すると思われる。

KI0023B と構造 20 との間の連結は、構造 21 に沿って伸びていると思われる。構造モデルにおいては、構造 21 の KA2563A-5 への連続が仮定されている。構造 21 が水み

ちであるか否かは明らかではないが、このゾーンは構造20での揚水に明らかに応答する。'99年3月のモデルではKI0025Bにおける構造21の構造19との交差が推定されている。構造21がここまで伸びているとの証拠は得られていない。

構造21および22の存在の実証における難点として、これらが試錐孔の他の主要ゾーンに非常に近接している点が挙げられる。構造22の存在確認試験の一例としてKI0025F02の掘削記録の調査があり、これによれば構造22は構造20から数メートル単位で分離し得ると考えられる。掘削記録の調査からその位置における構造の存在が肯定され、かかる構造が構造20に水理学的に密接に結合していることが示された。構造22は構造20から遠方へ伸べている様子はない。なぜなら、KI0023BまたはKA2563Aに見られるこの特徴の水理学的交差が存在しないからである。番号表示されていない構造についても、構造22を含むものに隣接する区間内において同定された。この特徴はKI0025F02に認められ、FI0025F02-6の構造22とKI0025F02-8の構造6につながっている。

構造6も構造モデルにおいて確認されているようではあるが、構造20ネットワークへの連結強度がKI00023B-7区間内でのショートサーキットにより過大評価されている可能性がある。この区間は構造20および6を含み、周辺条件および揚水条件の下で実施された希釈試験により試錐孔に沿ったショートサーキットの存在が確認されている。ゾーン6と構造20または21のいずれかと関連する水みちとを含むKA2563-5にも、同様のショートサーキットの存在の可能性がある。

構造19は水理学的には若干独立した構造であるが、KI0025F02-2をソースとして使用した短期圧力干渉試験により、その貫通性についても確認がなされている。構造19は、PT-2予備試験におけるKA2563A-1でのトレーサー希釈試験以外では、トレーサー予備試験のターゲットではなかった。この試験では、KI0023B内の構造21から揚水し、KA2563A-1における流速の変化が示された。またこのゾーンは構造19の他セクションよりもより強度な干渉応答を示した。先のKA2563Aパッカー・システムの設置によって、ゾーン1とブロック中央部分とを連結する人工的な水みちが形成されたとすれば、ピエゾメーターの設置の見直しが有益であろう。

構造20、21および22を連結する可能性のある他の二つの構造が干渉応答から同定された。そのうちの一つは連結構造22として既に言及されている。他の一つは約75メートルの深度においてKI0023B-5と交差し、構造13と構造20とを連結している可能性がある。

結論として、'99年3月の構造モデルは確証されると共に洗練されるに至っている。構造13および22は共に短縮されている。構造21については未だ不確定である。構造13と構造20との間の水理学的連結は十分に文書化されているが、これら二つの変化点間に水みちをもたらす構造の位置の特定は確実性を伴うものではない。構造20と構造6との間の追加的な水みちの定義から、本計画においてこれら二つの変化点間でのトレーサー試験の実施が検討されるべきことが示唆される。

チャネルネットワークモデル

1999年、GOLDER社は広範囲にわたるチャネルネットワークモデリングを実施した。モデルでは、(a)構造モデル開発における援助、(b)FIZの理論的考察を通じてのトレーサー試験設計の支援、(c)水理学的干渉およびトレーサーの各試験であるPT-1からPT-4の解釈の援助、および(d)シミュレーションと測定値との比較による構造モデルの確証の援助が実行された。

チャネルネットワークモデリングではFracMan/PAWorksソフトウェアが使用され、このソフトはTask5およびTask4の各シミュレーションにおいても使用された。TRUEブロックスケールでは、一連の構造モデルがそれらが開発された際に実行され、異なる試験境界条件が組み入れられた。図8にはチャネルネットワークモデルを図示する。この図には、500mスケールで与えられた広域スケールの境界条件への連結と、周辺微小割れ目および構造モデル番号が付与された構造からなる詳細なパイプ・ネットワークとがモデルの中央に示されている。

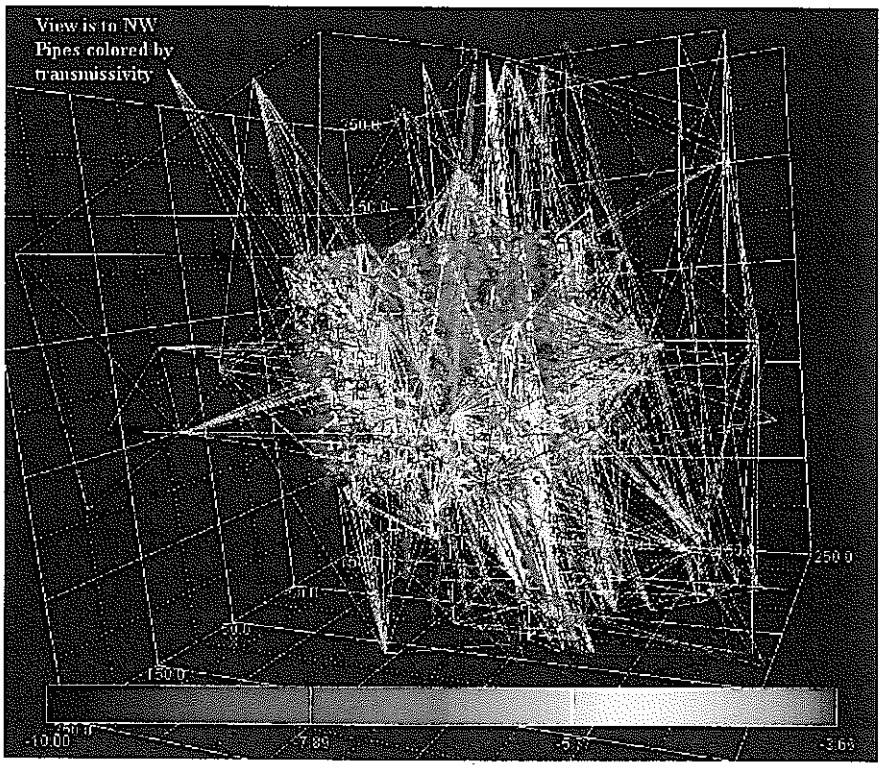

図8：PAWorksチャネルネットワークモデル

図9に、JNCチャネル・ネットワーク・モデルで実施された予備試験シミュレーションと予備試験2における水理学的干渉との比較の一例を示す。TRUEブロックスケール構造モデルに基づく調整済JNCチャネル・ネットワーク・モデルでは、観測された干渉挙動への適合が良好である。

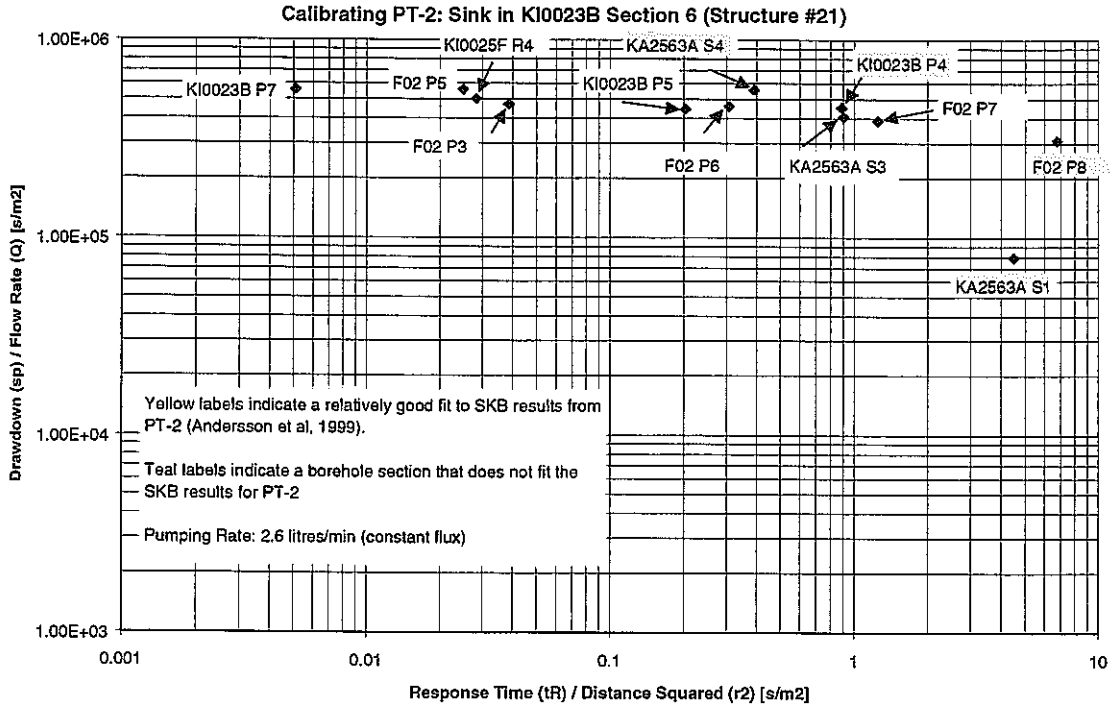

図 9：PT-2 予備試験に対するチャネル・ネットワーク・モデルの調整

フェーズ A のチャネル・ネットワーク予測

1999 年、Golder 社はトレーサー・テスト試験（TTS）のフェーズ A 用のトレーサー予測の為に一連のシュミレーションを実施した。このシュミレーションは、FracMan/PAWorks チャネル・ネットワーク（CN）モデルを用いて実施された。フェーズ A 用の チャネル・ネットワーク 予測は、フェーズ A のテスト A-1、A-2、A-3 及び A-4 の詳細な調整シュミレーション並びにテスト A-5 におけるトレーサーの破過予測を含んでいる。図 10 は、テスト A-5 における吸着及び非吸着トレーサーの注入時間の経緯を示している。

PAWorks による CN 予測のシュミレーション結果を図 11 から図 13 までに示す。図 11 は試験中の距離と水位低下の関係を示している。図 12 は、試験中のモデル領域における水圧の分布を示している。図 13 は、破過曲線の予測を示している。破過の統計は、表 2 に要約されている。

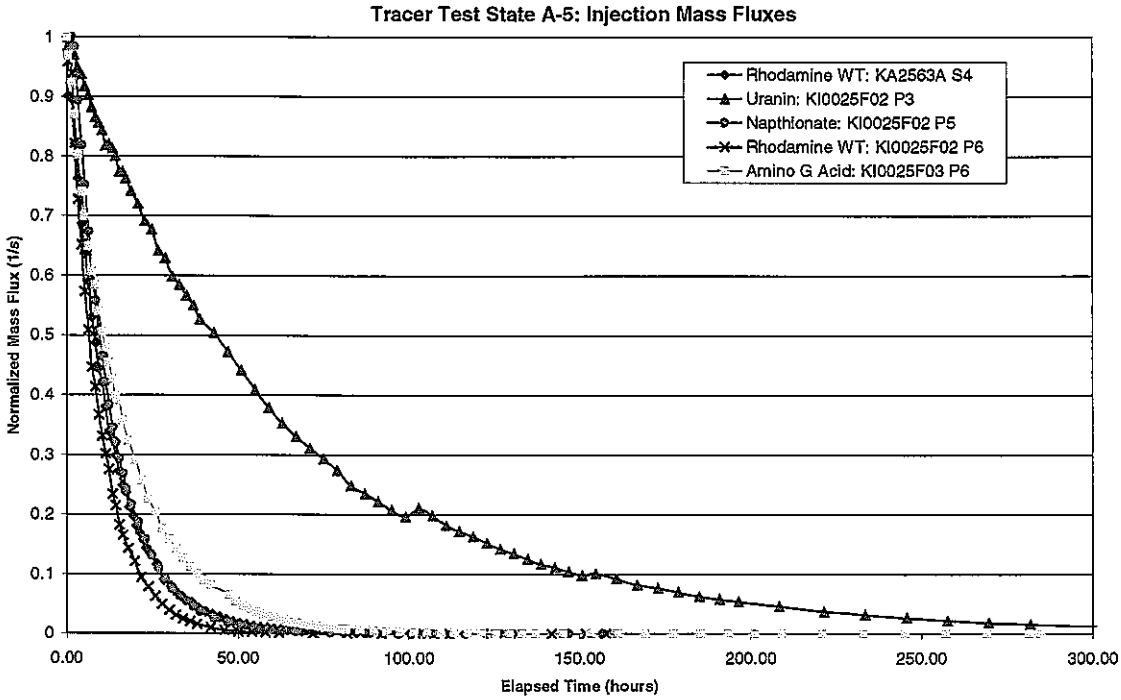

図 10：フェーズ A-5 トレーサー・テストの注入時間の経緯

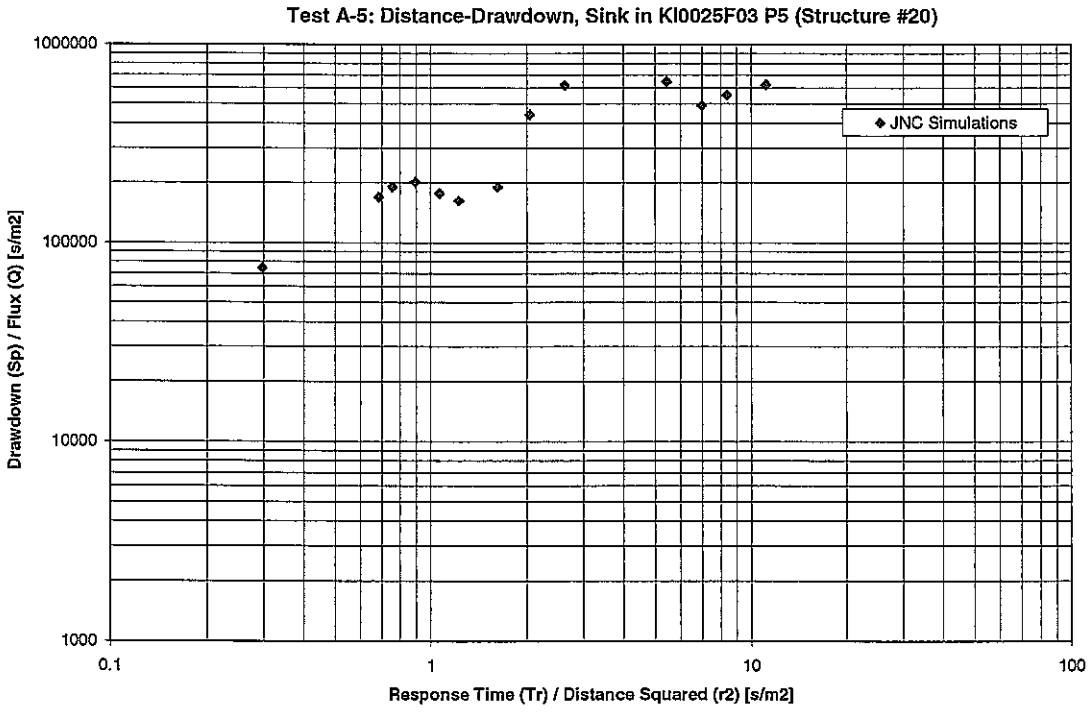

図 11：フェーズ A-5 トレーサー・テストの距離と水位低下の関係

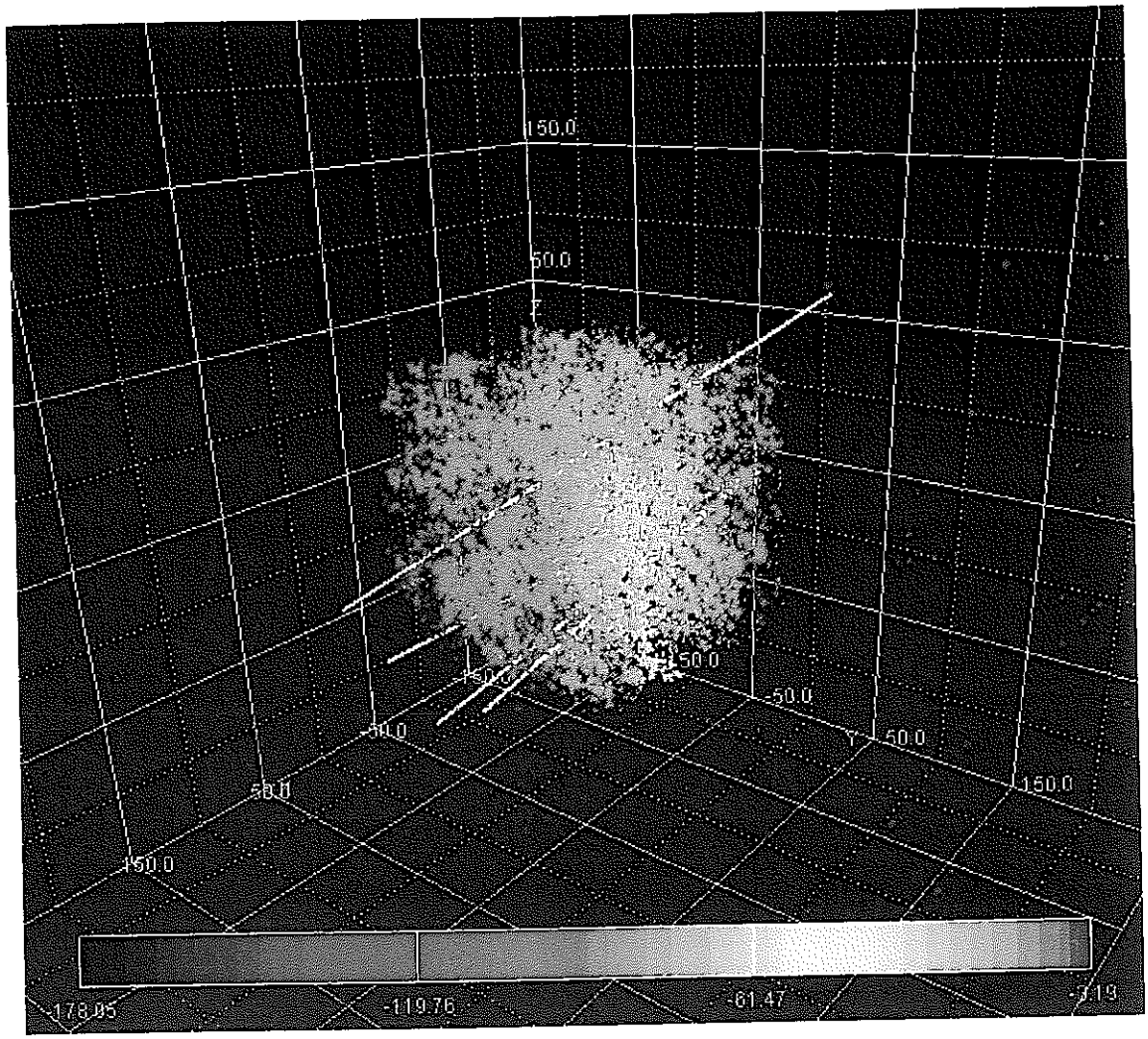

図 12：フェーズ A-5 トレーサー・テストの水圧の分布

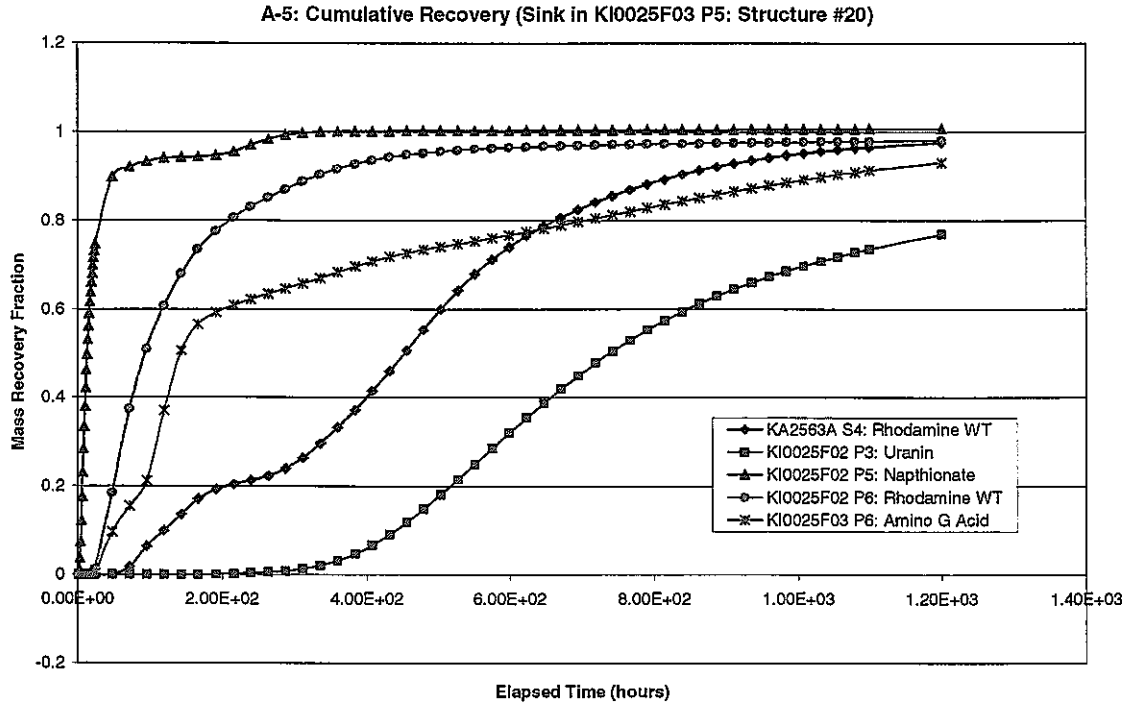

図 13：フェーズ A-5 トレーサーの破過予測

表 2：フェーズ A-5 予測

Species	T5 (hrs)	T50 (hrs)	T95 (hrs)
Rhodamine WT (1)	94	456	1008
Uranin	384	744	*
Napthionate	3.5	13	216
Rhodamine WT (2)	?	96	480
Amino G Acid	36	144	*

Golder Associates, Inc.

18300 Union Hill NE, Suite 200
Redmond, WA 98025
Telephone (425) 883-0777
Fax (425) 882-5498

Golder Associates

Report to:

Japan Nuclear Cycle Development Institute (JNC)
Tono, Japan

Version 0.01

TRUE Block Scale Project

Heisei-11
Progress Report

William Dershowitz
Thomas Doe
Aaron Fox

March 3, 2000

923-1089.1132
h11 true-bs report version 1.doc

TABLE OF CONTENTS

LIST OF FIGURES

LIST OF TABLES

1. INTRODUCTION

JNC participates as a full partner in the international Äspö TRUE-Block Scale experiment at the Äspö, Sweden Hard Rock Laboratory (HRL). This experiment is designed to advance the state of knowledge about flow and transport in less transmissivity fracture networks at the 50 to 100 m scale.

During HY-11, Golder Associates supported JNC participation in major aspects of the project, including,

- analysis of hydraulic, tracer transport, and fracture data
- theoretical studies of fracture intersection zones (FIZ)
- experimental design
- channel network model implementation and testing
- channel network flow and transport simulations

This report summarizes major achievements of Golder Associates support for JNC during HY-11. Golder analyses are described in detail in SKB Äspö Series reports prepared for the TRUE-Block Scale project. Reports prepared during HY-11 are listed in Table 1-1. These reports can be considered as attachments to this report, as they provide more detailed description of technical activities during HY-11.

SKB TRUE-Block Scale Report	Title	Date
ITD-99-XX	A CONDITIONAL DFN MODEL OF THE TRUE BLOCK SITE	April 99
ITD-99-XX	A PRELIMINARY CHANNEL NETWORK MODEL BASED ON THE SEPTEMBER 1998 STRUCTURAL MODEL	April 99
ITD-99-XX	SPATIAL DATA ANALYSIS	June 99
ITD-99-XX	TRACER PRE-TEST PREDICTIONS USING THE MARCH 1999 ASPO STRUCTURAL MODEL	June 99
ITD-99-20	RECONCILIATION OF THE MARCH'99 STRUCTURAL MODEL AND HYDRAULIC DATA	October 99
ITD-99-21	PATHWAYS ANALYSIS FOR FRACTURE INTERSECTION ZONE EFFECTS ON TRACER TEST DESIGN	October 99
ITD-00-03	CONDUCTIVE BACKGROUND FRACTURES IN THE AREA INVESTIGATED IN THE TRACER TEST STAGE (TTS)	January 00
ITD-00-XX	CHANNEL NETWORK MODEL PREDICTIONS FOR PHASE A TRACER TEST EXPERIMENTS	February 00

Table 1-1 TRUE-Block Scale Reports HY-11

2. TASKS

This section summarizes the tasks carried out by Golder Associates during HY-11. These activities are described in greater detail in the technical reports listed in Table 1-1. In addition to the technical activities described in technical reports, Golder supported JNC through

a) assisting JNC in developing project strategies to ensure that JNC obtains maximum benefit from TRUE-BS activities assistance;

b) coordinator, project task and schedules;

c) participating in project meetings; and

d) ensuring technology transfer from the TRUE-BS project to JNC staff at Tono and Tokai.

Table 2-1 lists the Äspö WBS activities included in the HY-11 scope. Short descriptions of the work carried out for each of these tasks are provided below. Detailed information is provided in the reports listed in Table 1-1

Äspö WBS	Task Title
3.3.5.2	Hydromodel Update/Tracer
3.3.5.5	Hydromodel Update/Reconciliation
3.3.6.3	Tracer Test Design/FIZ Study
3.3.6.4	Tracer Test Design/Specs
3.3.9.4	Channel Network 99.03 Model
3.3.10.1	DFN Technical Review
3.3.11.2	Tracer Test Design/CN Task Modeling
3.3.12.1	CN Modelling of Pre-tests
3.3.13	Modelling Workshop
4.2.3	Geometrical Analysis
4.2.11	Structural Model Update
4.5.2	CN Prediction for Phase A
4.5.4	Compilation and Analysis of Background Fracturing
4.5.5	Virtual Packer Location
4.6.3	Tracer Test Evaluation, Phase A
4.6.4	Modeling Workshop
4.10.2	Calibration of CN Model, Phase A
4.16.5	Test Design and Structural Model Support

Table 2-1 Äspö WBS Tasks for Golder During HY-11

2.1 Task 3.3.5.2 Hydromodel Update/Tracer

Golder carried out the following analyses to assist in updating the hydrogeological conceptual model of the TRUE-BS rock block.

- interpretation of well tests,
- interference test analysis,

- Posiva hydro-physical flow log analysis, and
- analysis of the geometry and geology of major numbered structures.

JNC assisted the TRUE Block Scale Project team in developing an appropriate hydro-structural model for the rock block which will be the focus for the tracer test stage (TTS), This required analsyis of hydraulic data sets including 5-m packer flow logs (KI0023B, KI0025F), Posiva flow logs (KI0025F02, KA2563A), pressure build-up tests (KI0023B, KI0025F02), pressure interference tests, drilling flow and pressure responses, and tracer dilution tests. JNC places particular emphasis n the pressure interference and dilution test results for the first three tracer pretests. Three pretests were used as sources representing structures 13 (KI0023B-3), structure 21 (KI0023B-5), and structure 20 (KI0025F02-5).

Tracer test design activities on the region around two numbered features, structures 20 and 13. The main tool for analyzing pressure responses has been plots of drawdown versus distance, divided by the distance between the observation point and the pumping source squared. The extent to which these points lie on coherent type curves or tend to cluster provides indications of the homogeneity of the system or the presence of multiple conductors. Maps of drawdown for each pumping test complement these plots. Figure 2-1 shows the boreholes analysed in the TRUE Block Scale rock block. The structural model is shown in Figure 2-2.

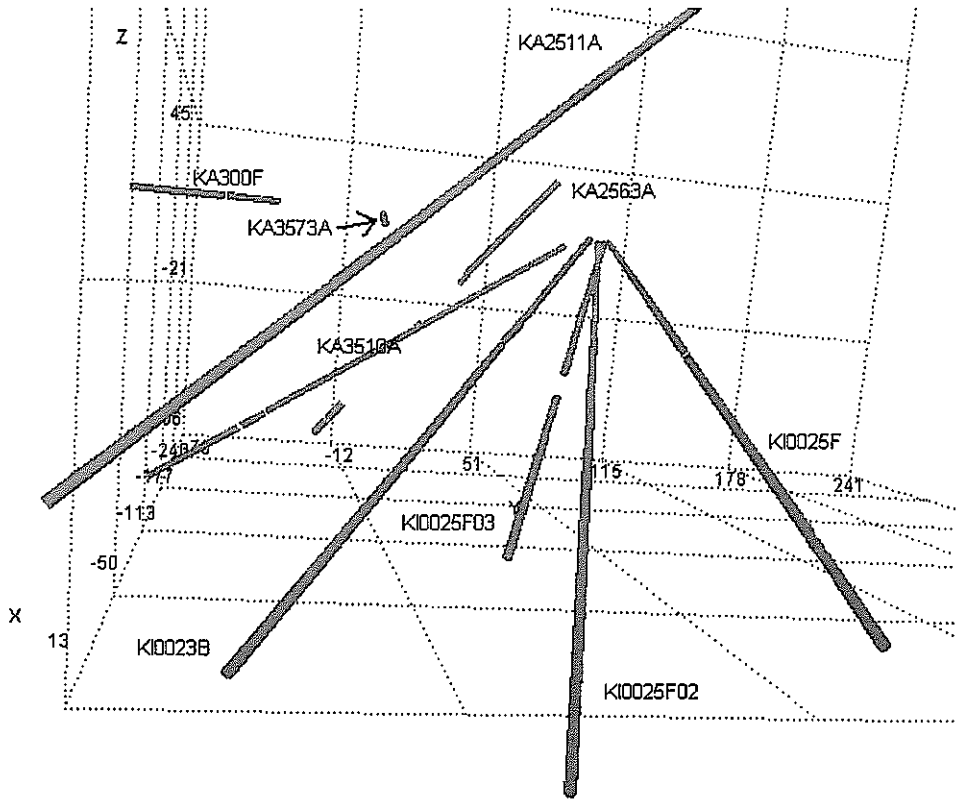

Figure 2-1 TRUE Block Scale Boreholes

The results of the reconciliation study have shown that the March '99 structural model provides a largely accurate description of the major conducting features in the TRUE block. A brief description of each feature is given below. A summary plot of the hydraulic data and the connectivity of the structures are shown in Figure 2-3. This figure shows the boreholes as parallel features for convenience of plotting data. The length axis is adjusted so that "0" is the location of Structure 20. This adjustment aligns the boreholes to allow a visual comparison of features common to different holes.

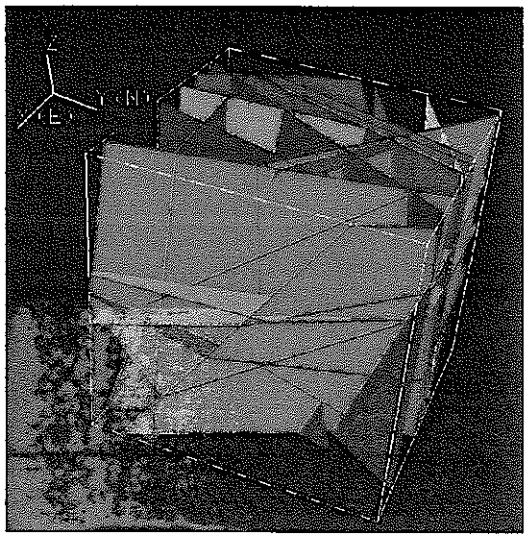

• 27 Fractures, colored by transmissivity

• External boundary is 500m x 500m x 500m

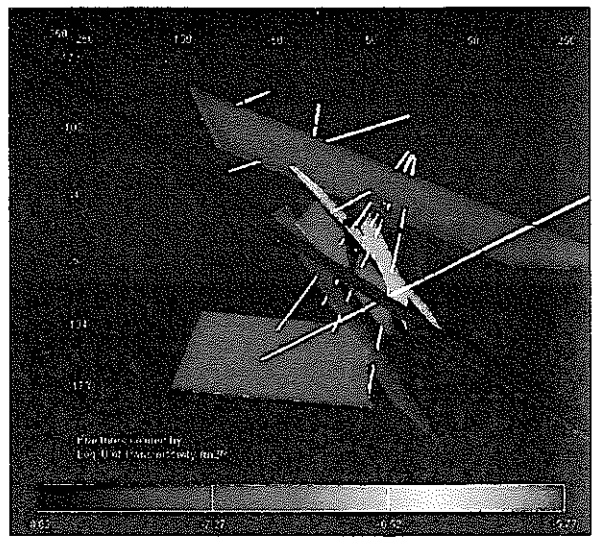

• 9 fractures modified in October 1999 structural reconciliation report

Figure 2-2 TRUE Block Scale Structural Model

Flow log anomalies and pressure buildup data are shown as bars with heights proportional to the inferred steady flows from those zones. The 5-m flow log data are shown as bar charts, and the locations of significant inflow or pressure response during drilling are shown with triangles below the line representing each hole. Each horizontal line on the chart represents a borehole. Packer locations are shown by squares, and heavier lines note the intervals that are being monitored. The March '99 structural model is shown in yellow, and inferred conductors from the recent data are shown as transparent gray overlays.

Structure 20 is the major conducting feature of the core of the block, and it appears in all boreholes except KA2511A, which lies about 80 m above the borehole array. The current pretests provide further validate the location and transmissive nature of Structure 20.

Structure 13 is distinct from but connected to Structure 20. The pressure responses in 13 indicate strong connections between boreholes KI0023B and KA2563A. The connection becomes weaker in KI0025F02 as the pressures respond later and with lower drawdowns. Structure 13 may largely disappear hydraulically between KI0025F.

The expected intersection of Structure 13 with KI0025F02-3 appears to have stronger connections with Structure 20 than with structure 13, as shown by larger drawdowns in response to the PT-2 and PT-3 tests. This connection may continue to KI0025F-3.

The connection between KI0023B and Structure 20 may travel along Structure 21. Structure 21 is hypothesized to continue to KA2563A-5 in the structural model. This zone does respond to pumping in structure 20, though it is not clear if Structure 21 is the conduit. The March '99 model also extrapolates Structure 21 to intersect Structure 19 in KI0025B. There is no evidence for this extension of Structure 21.

One difficulty in verifying Structures 21 and 22 has been that they appear very close to other major zones in the boreholes. One test of the existence of Structure 22 was to examine the drilling records of KI0025F02, which should separate 22 from 20 by several meters. The investigation of drilling records did affirm the existence of a structure in that location, and showed that hydraulically it is closely tied to Structure 20. Structure 22 does not appear to extend very far from Structure 20, as there are no hydraulic intersections of this feature observed in KI0023B or KA2563A. Another structure, which has no number designation, was also identified in the adjacent interval to the one containing Structure 22. This feature appears in KI0025F02 and connects Structure 22 in FI0025F02-6 with Structure 6 in KI0025F02-8.

Structure 6 also appears validated in the structural model, however, the strength of its connections to the Structure 20 network may be exaggerated by a short circuit in the KI00023B-7 interval. This interval contains both Structures 20 and 6, and dilution tests performed under both ambient and pumped conditions confirm the presence of a short-circuit along the borehole. A similar short-circuiting may appear also in KA2563-5, which contains zone 6 and a conductor that may be associated with either Structure 20 or 21.

Short-term pressure interference tests using KI0025F02-2 as a source provide further validation of Structure 19 as a through-going, though somewhat isolated hydraulic structure. Structure 19 was not a target of tracer pretesting other than to perform tracer dilution tests in KA2563A-1 during the PT-2 pretest. This test pumped Structure 21 in KI0023B and showed a water velocity change in KA2563A-1. This zone also showed stronger interference responses than other sections of structure 19. Given that a previous installation of the KA2563A packer system had artifacts that created connections between zones 1 and the central part of the block, it may be useful to review the piezometer installation.

Two other structures that might connect Structures 20, 21, and 22 were identified from the interference responses. One was already mentioned above as connection structure 22. The other intersects K0023B-5 at about 75 meters depth and may connect 13 and 20.

In conclusion, the reconciliation efforts have both validated and refined the March '99 structural model. The reconciliation shortened both Structures 13 and 22. Structure 21 is still uncertain. The hydraulic connections between 13 and 20 are well documented, but the exact locations of structures carrying water between these two features are not know with great confidence. The definition of additional conducting features between Structures 20 and 6 suggest that the project consider including a tracer test in between these two features.

2.2 Task 3.3.5.5 Hydromodel Update/Reconciliation

During HY-11, Golder assisted JNC in integration of hydrogeological and geological information to develop an integrated hydro-structural model for the focus area of the TRUE-BS block. This summary describes work to reconcile the March '99 structural model with hydraulic data (Doe et al., in prep). The hydraulic data sets include 5 m double packer flow logs (KI0023B, KI0025F), Posiva flow logs (KI0025F02, KA2563A), pressure build-up tests (KI0023B, KI0025F02), cross-hole pressure interference tests, flow and pressure responses collected during drilling, and tracer dilution tests. Particular emphasis has been put on the cross-hole pressure interference and dilution test results for the first three tracer Pre-tests (PT-1 through PT-3). The three Pre-tests have used as sources; Structure #13 (KI0023B:P4), Structure #21 (KI0023B:P6), and Structure #20 (KI0025F02:P5), respectively.

An important task for tracer test design is the identification of conducting features that connect major structures. The major goal of the TRUE Block Scale programme has been to look at tracer behaviour along pathways involving multiple conducting features. The sub-parallel orientations of the major features in the block has complicated the search for a network of features, hence particular emphasis has been placed on finding verifiable conductors that cross the major NW Type 1 trending conductive structures.

The TRUE Block Scale Technical Committee decided to concentrate the tracer design activities on the region around two numbered Type 1 structures, Structures #20 and #13. Hermanson (in prep) in his draft report on the March '99 model, proposed two new Type 2 features that crosscut Structures #13 and #20, giving them the designations "#21" and "#22". This review effort seeks a verification and visualisation of the hydraulic data to check the existence of these features and others that may be suitable for tracer testing.

The main tools for analysing pressure responses have been plots of drawdown versus distance, divided by the distance between the observation point and the pumping source squared. The extent to which these plotted points lie on coherent type curves or tend to cluster provides indications of the homogeneity of the system or the presence of multiple conductors. These plots are complemented by maps of drawdown for each pump test. Figure 2-4 shows an example of a distance-drawdown plot for the PT-3 test.

The results of the reconciliation study have shown that the March '99 structural model provides a largely accurate description of the major conducting features in the TRUE Block Scale volume. A brief description of each important structure is given below. A summary plot of the hydraulic data and the connectivity of the structures is shown in Figure 2-3. This figure shows the boreholes as parallel features for convenience of plotting data. The length axis is adjusted so that the origin "0" is the location of Structure #20. This adjustment aligns the boreholes to allow a visual comparison of features common to different holes.

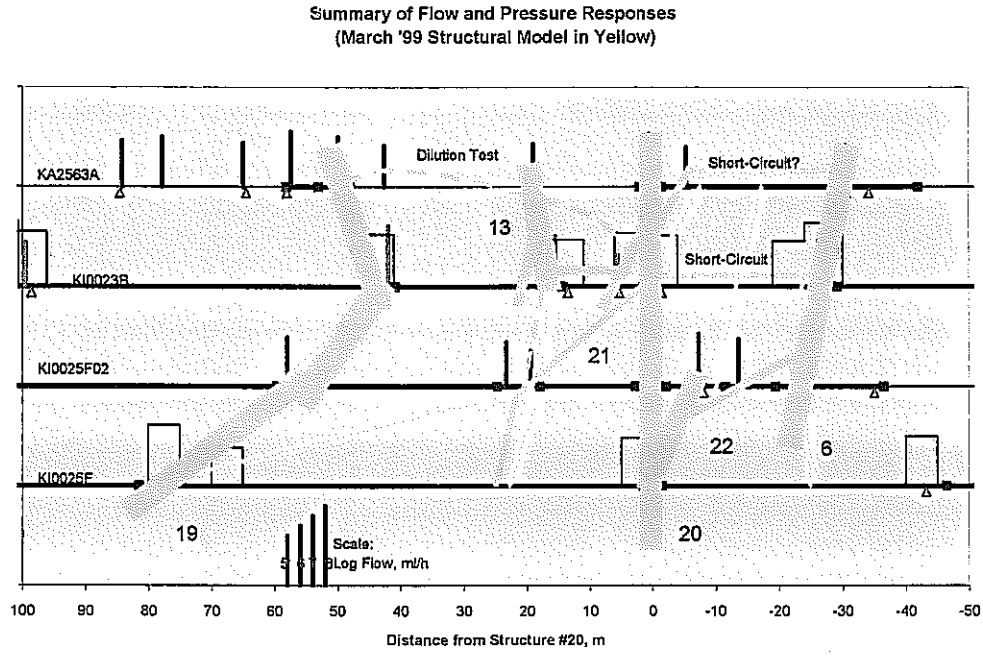

Figure 2-3 Reconciled hydraulic and structural model of the TRUE Block Scale volume. Grey shaded lines show hydraulic structures. Yellow lines indicate structures in March '99 Structural model.

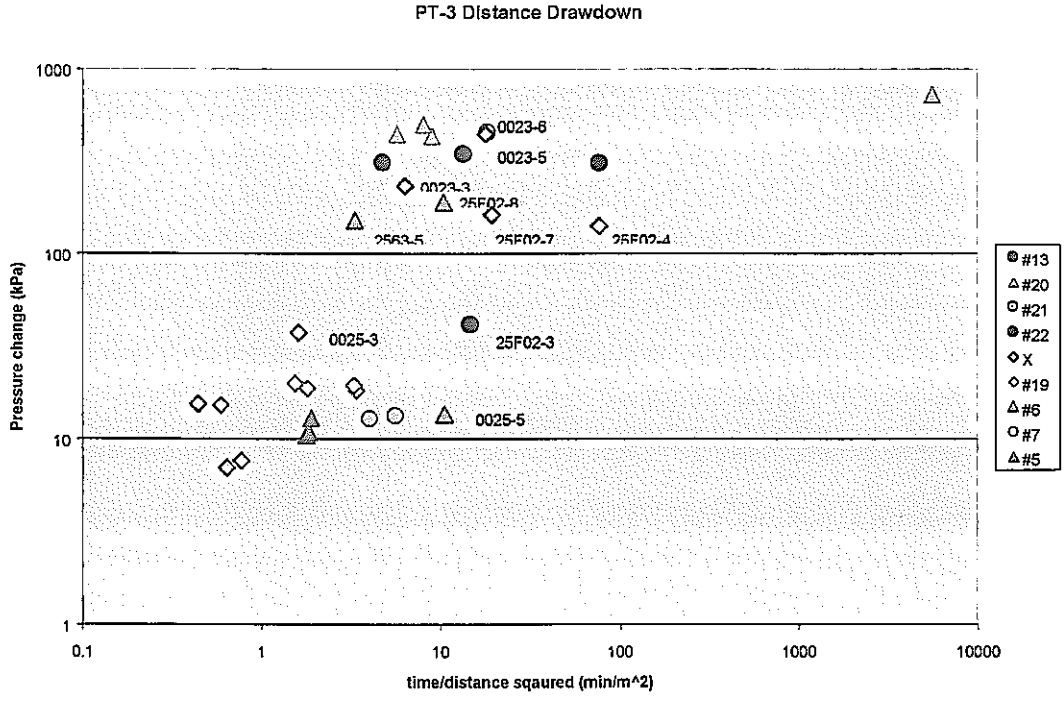

Figure 2-4 Example Drawdown Distance plot for PT-3.

Flow log anomalies and pressure build-up data are shown as bars with heights proportional to the inferred steady flows from those zones. The 5-m flow log data are shown as bar charts, and the locations of significant inflow or pressure response during drilling are shown with triangles below the line representing each hole. Each horizontal line on the chart represents a borehole. Packer locations are shown by squares, and heavier lines note the intervals that are being monitored. The March '99 structural model is shown in yellow, and inferred conductors from the recent data are shown as transparent gray overlays.

Structure #20 is the major conducting feature of the core of the block, and it appears in all boreholes except KA2511A, which lies about 80 m above the borehole array. The current pre-test results provide further validation of the location and transmissive nature of Structure #20.

Structure #13 is distinct from, but connected to Structure #20. The pressure responses indicate strong connections between boreholes KI0023B and KA2563A. The connection becomes weaker in KI0025F02 as the pressures responses are later and lower in magnitude. The responses of KI0025F02:P3 are very important for the hydraulic model. The March'99 structural model also has Structure #21 intersecting in this zone. It is significant that this section responds weakly to all three Pre-tests, and even more weakly to pumping in Structure #13 than to Structures #20 and #21. An alternate explanation for the low drawdown in KI0025F02:P3 is a boundary effect. than Structure #13 such that it provides a stronger flow than we would expect from Structure #13 alone. A boundary effect that would cause a reduced drawdown would imply a constant-pressure rather than a no-flow boundary. Constant-pressure boundary effects imply that the interval contains a second conductor with higher storage and conductivity. We can discriminate between these two possible explanations, poor connection versus boundary effect by checking the dilution data. If the connection is poor, we should see low-flow results in tracer dilution test from this interval, while a boundary effect would show stronger dilution. Dilution tests indicate that there is a Structure #13 connection and the low drawdown may therefore be a boundary effect.

Structure #13 may largely disappear hydraulically between KI0023B and KI0025F02.

One difficulty in verifying Features #21 and #22 has been that they appear very close to other major zones/structures in the boreholes. One test of the existence of Feature #22 was to examine the drilling records of KI0025F02, which should separate #22 from #20 by several metres. The investigation of drilling records did affirm the existence of a structure at the assumed location of #22, and showed that hydraulically it is closely tied to Structure #20. Structure #22 does not appear to extend very far from Structure #20, as there are no intersections of this feature observed in KI0023B or KA2563A. Structure #22 also extrapolates to intersect Structure #19 in KI0025F in the March'99 structural model (Hermanson, in prep). There is however no hydraulic evidence for this extension of Structure #22.

In the pressure interference responses of the pre-tests, Structure #22 (KI0025F02:P6) behaves as an integral part of the Structure #20 network. This feature is also interpreted to act as part of the bridge from Structure #20 to Structure #6. The feature does not extend to the northwest, as there appears to be no flow anomalies along the projections of the structure in KA2563A or KI0023B.

The pressure interference data and the tracer dilution data offer somewhat contradictory evidence for Feature #21. The tracer dilution data for Pre-test PT-2 show a clear connection between KI0023B:P6 and KI0025F02:P3. The pressure interference tests do not indicate a strong hydraulic connection between KI0025F02:P3 and other proposed Structure #21 locations. The

most striking aspect of the pressure behaviour of KI0025F02:P3 is its generally low-pressure response. When discussing Structure #13 above, this low-pressure response was explained as a possible boundary effect where Structure #21 was acting as a very permeable boundary that reduced the pressure responses to pumping in Structure #13. By this logic, Structure #21 should be more transmissive than Structure #13 and pumping in Structure #21 at KI0023B:P6 should produce stronger drawdowns in KI0025F02:P3 than pumping in Structure #13, as was done in Pre-test PT-1.

Unfortunately for clarifying the hydraulic structure, PT-2 produces only slightly stronger drawdowns in KI0025F02:P3 than PT-1 did. There are clearly connections between KI0025F02 and Structure #20, but these do not support a very direct connection along a possible Structure #21.

One could look for another candidate intersection of Structure #21 in KA2563A:S5. This zone contains a conductor at the right location, but sharing a piezometer interval with Structures #6 and #7 may smear its pressure responses. KA2563A:S5 does have strong drawdown, but the behaviour is consistent with the responses of other parts of Structure #6.

In summary, the evidence for Feature #21 mainly comes from geology and the tracer dilution test results. The dilution tests performed as part of PT-2 support a pathway along the proposed feature, whereas the hydraulic pressure interference data do not suggest a strong hydraulic pathway.

Another structure, which has no designated number, was also identified in the adjacent interval to the one containing Feature #22 in borehole KI0025F02. This feature appears to connect Structure #22 with Structure #6.

Structure #6 as presented in the structural model appears validated, however, the strength of the connections may be exaggerated by a short circuit in the KI0023B:P7 interval. This interval contains both Structures #20 and #6, and dilution tests performed under both ambient and pumped conditions confirm the presence of a short-circuit along the borehole.

Section KA2563A:S5 contains two significant conductors at 157.6 and 182.6 m. The shallower interval is part of Structure #6. The deeper interval is has not been identified with any numbered conductor, but it may be part of the Structure #20 system as it is separated from the main trace of Structure #20 by only 6 metres. However, the two structures at L=182.6 m are associated with two subhorizontal structures (225/11 and 244/15), but could still potentially connect to Structure #20 at L=188.7 m. If the 182.6 m conductor is part of the Structure #20 system, then it may be acting as a short circuit similarly to what has been found KI0023B:P7. It should however be noted that the transmissivity of the structures concerned are significantly smaller (10-50 times). Given a head difference of 5 m, the resulting "leakage flow" is about 0.2 l/h, which should be compared with the 10 l/h flow calculated for the KI0023B:P7 short circuit. Consequently the effect of this short-circuit, if it does exist, will be significantly lower than the one in KI0023B:P7.

It was recommended that KA2563A:S5 should be a target for dilution tests to measure the flow rate under both natural and, if possible, pumped conditions. If this section has a significant flow, it may be desirable to install a packer at about 170 m in KA2563A.

Short-term pressure interference tests using KI0025F02:P2 as a source provide further validation of Structure #19 as a through-going, though somewhat isolated hydraulic structure. Structure

#19 was not a target for the pre-tests other than to perform a tracer dilution test in KA2563A:S1 during PT-2 and an actual tracer injection in the same section during PT-4, cf. Chapter 5. The former test (PT-2) pumped Structure #21 in KI0023B and showed a water velocity change in KA2563A:S1. This zone also showed stronger interference responses than other sections containing the interpreted Structure #19. Given that a previous installation of the KA2563A packer system produced artifacts, i.e. a created connections between the innermost section and the central part of the block, it may be useful to review the piezometer installation.

Two other structures that might connect Structures #20, and Features #21 and #22 were identified from the interference responses. One was already mentioned above as a connection to Feature #22. The other one intersects KI0023B:P5 at about 75 meters depth and may connect Structures #13 and #20.

2.3 Task 3.3.6.3 Tracer Test Design/FIZ Study

Golder carried out extensive sensitivity studies using FracMan/PAWorks software to assist in design of tracer tests which are able to detect influences of fracture intersection zones (FIZ).

The basic model used for the generic study consists of two fractures that intersect each other, cf. Figure 2-5. Both fractures contain a number of random flow channels. At the intersection of the two fractures a FIZ exists, which builds a deterministic flow channel. Both fractures are also intersected by two wells. The intersections are isolated with packers, so they can be used as test intervals.

If tracer is released at the source location it will travel through the flow channel network on the first fracture towards one of the sink intervals. If the sink interval is on the second fracture the tracer will travel a certain distance along the flow channel built by the FIZ before entering the flow channel network on the second fracture. The exact pathway, and therefore the portion of the pathway within the FIZ, is a function of the (random) location of the flow channels and of the packer interval configuration.

If gravity effects are ignored, the flow channel network built by the two fractures shown in Figure 2-5 can be modelled in two dimensions. The resulting conceptual model is shown in Figure 2-5 and the rectangular grid representation in Figure 2-5.

The channel network model used in this study combines, cf. Figure 2-5;

- deterministic elements (the fractures, the FIZ and the packer intervals)
- stochastic elements (the channels).

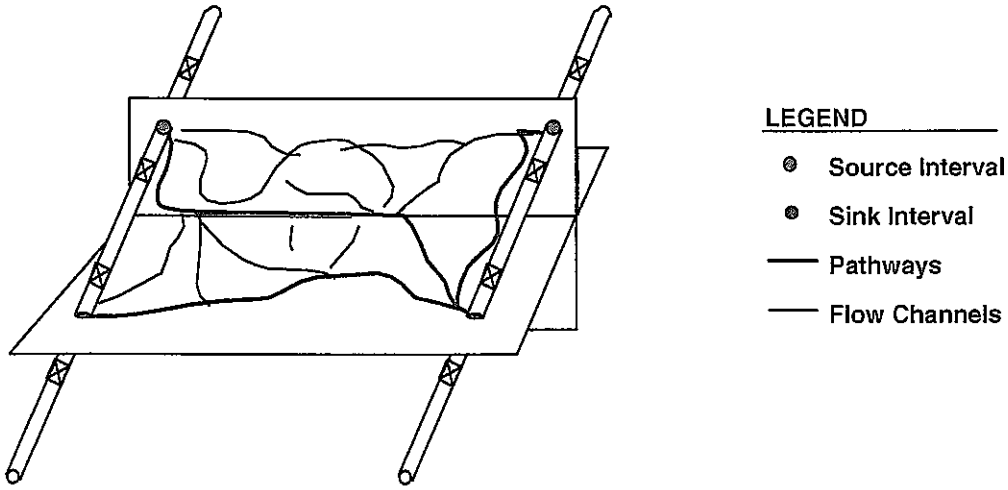

Figure 2-5 Generic F12 Conceptual Model

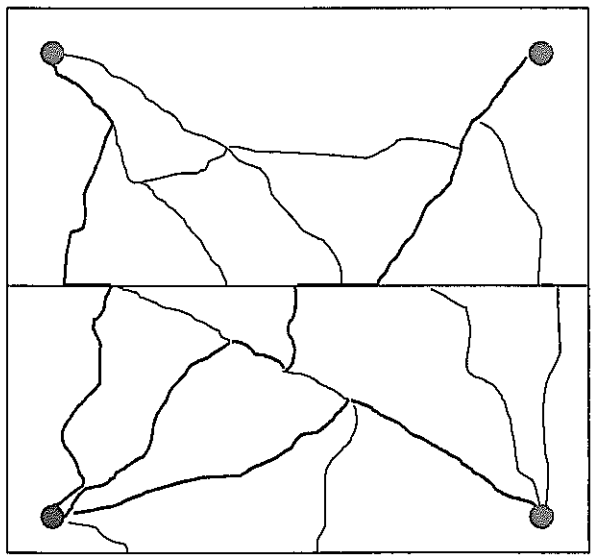

Figure 2-6 Two Dimensional View of Generic F12 Conceptual Model

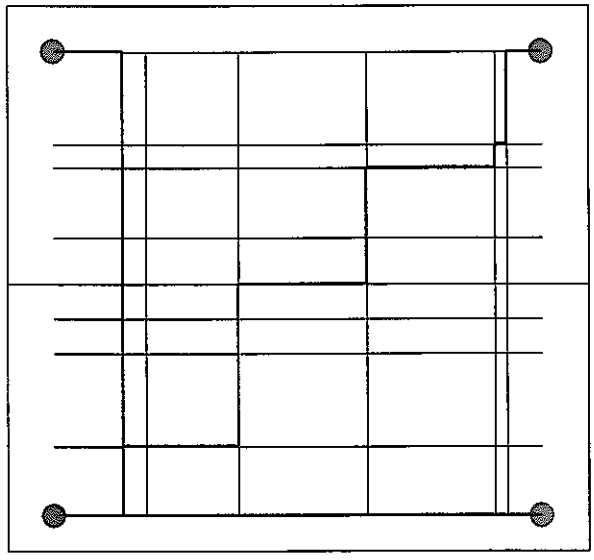

Figure 2-7 Generic F12 Channel Grid Model

Channel Network Model

The model region is 100 x 100 m. The transmissivities of the channels are assigned stochastically based on the defined transmissivity distribution. Ten realisations of the fracture network were generated. Channel apertures were calculated using the following equation: $e = 2\,T^{0.5}$. The simulated tracer test was designed as an equal strength dipole test. The model contains one source zone, which is injecting water at a constant head of 10m, and a sink zone, which is withdrawing water at a constant head of –10m. All intervals are at a distance of 48.5 m from the FIZ.

Simulation strategy

The main purpose of the simulations was to investigate under which circumstances the FIZ can be 'seen' by tracer tests. As mentioned above, the properties of the FIZ can not be measured directly by *in-situ* experiments, but only in combination with the properties of the overall fracture network. Thus a single tracer test is not sufficient to assess the properties of the FIZ.

However, the simulations allow us to test the hypothesis by comparing results from multiple simulations. By locating well pairs in a certain way, it is possible to generate pathways between well pairs with very different portions of the total pathway length affected by the FIZ. To assess the effect of the FIZ, the minimum travel time for these three different well pairs was computed for:

- Pair 1: Parallel to FIZ
- Pair 2: Perpendicular to FIZ
- Pair 3: Diagonally and across the FIZ

For pair 1 the shortest pathway lies completely outside the FIZ. The flow field during a dipole test (and with it the tracer travel time), however, will be affected by the FIZ. For pair 2, the tracer travel time will be affected the least by the FIZ, because the all flow lines will cross the FIZ

perpendicularly. For well pair 3, the flow field will be affected by the FIZ, and a large portion of the pathway fails within the FIZ.

Transmissivity Models

The ability to "capture" the FIZ will largely depend on the transmissivity contrast between the FIZ and the surrounding flow channel network. To study this aspect the following four different pipe network cases were generated an analysed:

- Case 1: Homogeneous pipe network, where all pipes including the FIZ have the same transmissivity ($1,10^{-08}$ m^2/s)
- Case 2: Homogeneous pipe network with increased transmissivity for the FIZ ($1{\cdot}10^{-3}$ m^2/s), ie. a five order of magnitude difference.
- Case 3: Heterogeneous pipe network, where the pipe transmissivities are random (Normal of Log distribution) except for the FIZ. Transmissivity for the FIZ equals mean of transmissivity distribution ($1{\cdot}10^{-8}$ m^2/s)
- Case 4: Heterogeneous pipe network, where the pipe transmissivities are random except for the FIZ. Transmissivity for the FIZ is greater than mean of the transmissivity distribution ($1{\cdot}10^{-3}$ m^2/s)

Cases 1 and 2 assume a homogeneous flow channel network. In Case 1, it is also assumed that the FIZ does not have an increased transmissivity with respect to flow channels in other areas of the fracture. In Case 2 the FIZ transmissivity is increased in comparison with the transmissivity of the flow channels.

For Cases 3 and 4 it is assumed that the transmissivity along the flow channels varies significantly (Normal of Log distribution with standard deviation of $1{\cdot}10^{-2}$ $m^2/$). In Case 3 the assumption is that the FIZ has no increased transmissivity compared to the flow channels in other areas of the fracture, while Case 4 assumes an increased transmissivity along the FIZ.

Results

The simulations include a pathway search which minimizes the overall travel time between the source and the sink interval. The search was carried out for all 10 generated realisations for each case. Table 2-2 shows the results for the four cases modelled and the three assumed well pair setups.

Model	Travel Time, hours		
	Diagonal	Perpendicular	Parallel
Case 1: Homogeneous	5500	1053	1467
Case 2: Homogeneous with increased T for FIZ	6750	1064	1681
Case 3: Heterogeneous	5333	2481	2805
Case 4: Heterogeneous with increased T for FIZ	10278	2742	5861

Table 2-2 Calculated shortest travel time pathways (base cases 1-4)

Table 2-2 shows that an increased transmissivity in the FIZ causes an increase in the smallest travel time for all well pairs. This is probably caused by the larger fracture aperture that is assumed in the model for fractures with an increased transmissivity. The larger aperture causes a slower flow velocity and thus, a longer travel time.

Surprisingly, a FIZ with a higher transmissivity is almost 'invisible' in a homogeneous channel network. The travel times are similar for both cases, with or without the increased transmissivity in the FIZ.

For a heterogeneous channel network, the effects of the increased transmissivity in the FIZ are more apparent. The smallest travel time doubles for the parallel and the diagonal well pairs. Only the perpendicular well pair (which was not expected to be influenced by the FIZ, anyway) shows similar travel times.

Model variations and sensitivity studies

The above model cases were rerun with a situation where the test sections are located 15 m from the FIZ (compared to 48.5 m in the modelled bases cases). The results indicate that a shorter distance will increase the possibility to 'capture' the FIZ.

The homogeneous base cases were rerun with a factor 2.5 higher density of flow channels (50 fractures compared to 20 in the base cases). No significant difference compared to the base cases was observed.

The cases with a 15-m distance between the test intervals and the FIZ were rerun with increased and decreased transmissivity contrast. No significant differences were observed compared to the results of the above variation runs.

2.4 Task 3.3.6.4 Tracer Test Design/Specs

Golder supported JNC in working with the TRUE-BS project team in

- defining tracer testing objectives consistent with the project goal for block scale fracture network sorbing tracer transport,
- determining the feasibility and efficacy of alternative designs, and
- defining tracer test configurations and specifications.

The characterization program has identified several major geologic structures that cut across significant portions of the site. These structures have been assigned numbers for identification. For the most part the numbered structures are those which appear in at least three boreholes with a high level of confidence. A subset of these structures are hydraulically significant on the basis of pressure interference results during drilling and cross-hole pressure interference tests. These Structures, #5, #6, #7, #20, #13, and #19, trend NW and have steep dips. Features in other orientations, both subvertical (e.g. #8) and subhorizontal (eg. #18), appear in single or multiple holes but are not hydraulically conductive, at least not at their intersections. Structures #1 through #5 are part of a wide, well connected system of conductors, with portions that

required grouting during some of the drilling operations, and are therefore not useable for tracer experiments. Thus the major features that will be the focus of the testing programme will be Structures #13, #20, and #19, cf. Figure 2-8.

2.4.1 Less well identified conductors (Type 2)

In addition to the major numbered structures, the TRUE Block Scale volume contains additional geologic features and conductors. These have so far gone un-numbered because they are not sufficiently extensive to appear in more than one or two boreholes. Although the numbered features have been the main focus of testing to date, Type 2 features will be important for forming the networks for tracer testing in the block. In the most recent update of the TRUE Block Scale structural model, two Type 2 features, #21 and #22, have been identified, cf. Figure 1-1. These features will become better identified as the program focuses on a smaller part of the TRUE Block Scale volume.

2.4.2 Identification of suitable conducting networks

The hydraulic and structural model of the TRUE block area provides a basis for designing the geometry of tests to study tracer transport and retention. The major objective of the TRUE Block Scale experiments is the study of the tracer retention in fracture networks. The tracer tests must therefore include pathways that pass through multiple fractures, or conducting features. In addition to these pathways, the tracer test programme should ideally include some pathways that are entirely within individual conducting features to provide a basis for distinguishing network behaviour from that of single features.

The tracer test designs will need to use both the well-characterised numbered structures of Type 1 and less characterised features of Type 2. The major candidate structures, #13, #19, and #20 are nearly parallel, hence it will be impossible to form a network with these conductive structures, cf. Figure 2-8. At one point Structure #9 was considered a potential feature that might provide for connection between the NW trending structures (Hermanson, 1998, Winberg, 1999). However, recent tests have confirmed that Structure #9 is not well defined and does not appear to be a conductor. Structure #19 is a well-defined conductive feature, but it appears to be relatively isolated in the upstream part of the investigated rock volume. Hence, the main focus of tracer test design has shifted to structures #13 and #20, which are 10-20 m apart and to the two Type 2 features, #21 and #22, which may provide hydraulic connections between the former two structures. Features #21 and #22 have been the in focus during the performed Pre-tests and the subsequent hydraulic reconciliation study.

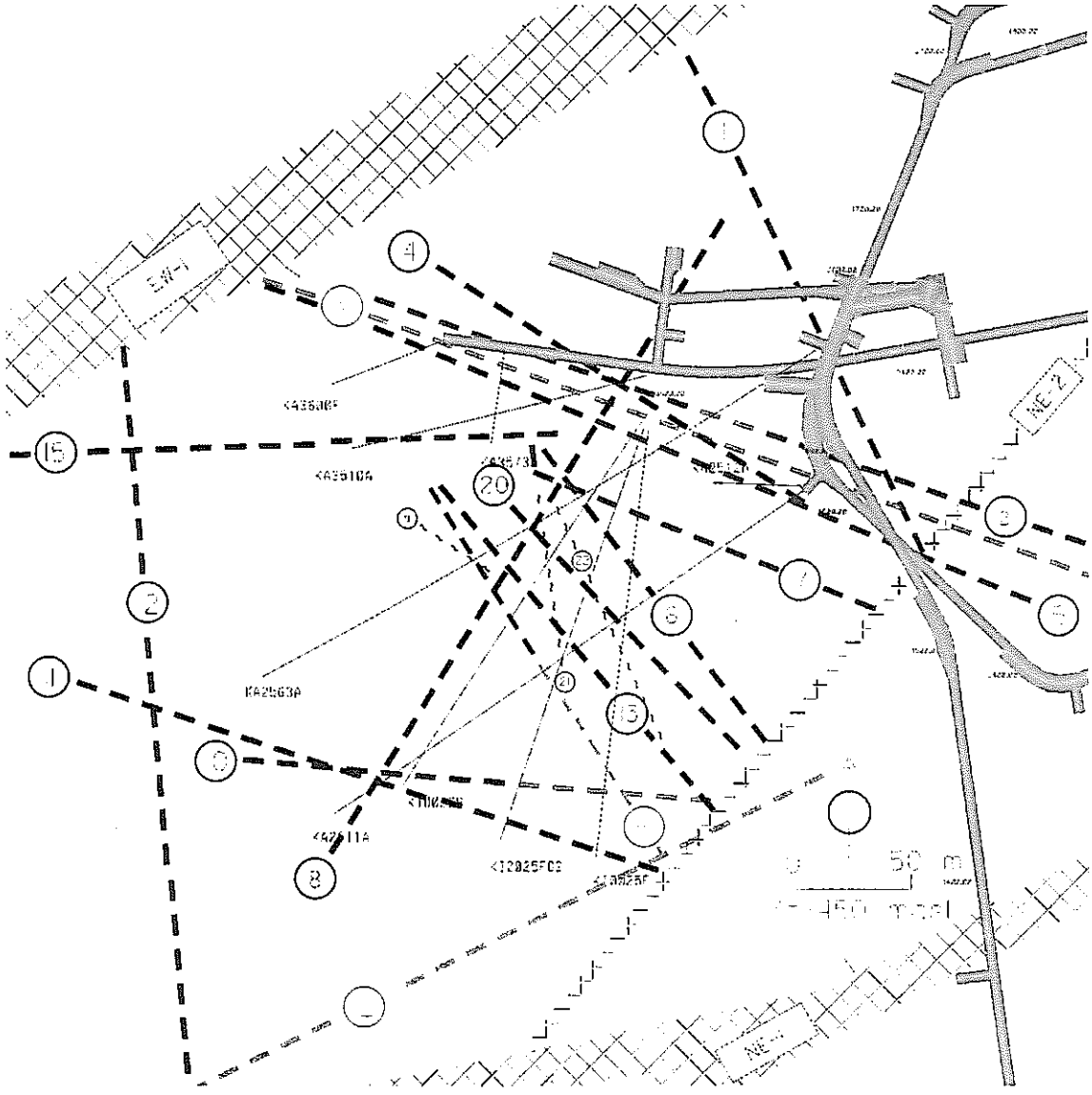

Figure 2-8 March 1999 structural model. Horizontal section at Z=-450 masl (Hermanson, in press).

2.4.3 Reality of performing tracer tests in networks

The poor recovery of many tracer tests in fractured rock is a fact. Most numerical models, on the other hand, predict complete recovery, whereas actual tracer tests generally fall short of that goal, or may show no recovery at all.

The poor recovery of tracers may reflect problems in the experiment design, lack of information about hydraulic geometry, or the effects of active fundamental transport processes. It is vital that we learn how to distinguish between these three factors. We wish to eliminate artifacts of the

test design and ignorance regarding flow geometry as much as possible so we can concentrate on transport processes.

The question of poor recovery leads to several hypotheses including:

- Tracer recovery is affected by background flow.
- Tracer recovery may be affected by accidental injection into stagnant areas of the flow system.
- Tracer recovery may reflect multiple complex pathways, such as:
  - ! Tracers following unexpected, and long pathways,
  - ! Dilution due to intersections providing additional water sources along a tracer transport pathway, making it difficult to actually measure the tracer concentration, and
- Tracer recovery may reflect strong matrix interaction effects.

Of these issues the background flow is mainly a design issue. Background flow should be known and understood and compensated for at the design stage - we should not use the tracer test to measure the background flow! The second and third hypothesis issues are partly design and partly process issues. The complexity of pathways, including the existence of dead-end or stagnant portions of the networks, is important to know to completely understand the resulting pathways. However, we should have some idea whether we are likely to encounter simple, complicated, or multiple pathways before tests are run. The performed tracer dilution tests are important in this context.

It should however be pointed out that a low tracer recovery, or even the lack of recovery, given a satisfactory understanding of the hydraulic geometry and a good tracer test design, may from the perspective of performance assessment, paradoxically, be a beneficial finding. This conclusion obviously has to be stated relative to the geological environment in which the test has been performed.

2.4.3.1 Effects of background flow

Tracer recovery is significantly affected by background flow in a fracture network. Background flow should be understood before testing by a combination of model simulations and measurements, such as by tracer point dilution measurements. One means of assessing background flow as a factor is to vary pumping rate at the withdrawal section. Clearly recovery should improve with a stronger sink. Background flow will, in conjunction with the transmissivities of the sink and source sections, also affect reciprocity (the change in breakthrough when the source and receiver are reversed).

2.4.3.2 Effects of diffusion in stagnant zones

Poor recovery may result when the tracer is accidentally introduced into a stagnant portion of the network, such as along a dead-end fracture. Such a stagnant area may have strong pressure responses to the pumping interval, but will not have a flow response due to the lack of

connection to a source of water. The risk of encountering such a situation can be reduced by performing a tracer dilution test prior to the actual tracer injection.

The lack of a water source means that dead-ends will have very low velocities both in tracer dilution measurements and in convergent flow test, where the tracer injection rates are minimal. Tracer breakthrough from a dead-end connection can be enhanced by switching from a convergent flow test (where the tracer is injected with minimal flow rate) to a dipole test (where tracer is injected at the same rate or some significant fraction of the pumping well withdrawal rate). The dipole test should provide a significantly improved breakthrough. Design tasks related to this issue should review existing dilution data and recommend additional tests to support design work. As in the previous tracer tests, preliminary dilution measurements are highly desirable. A review of pressure interference and point dilution behaviours may identify some dead-end zones. Dead end zones should have very strong drawdown behaviours that are distinctive in pressure interference tests.

2.4.3.3 Effects of pathway complexity

Poor recovery may reflect complexities of the pathways. In general, tracer tests that involve only a single fracture or feature may have better recovery than tracer tests in complicated networks, the latter type more prone to involve multiple complicated pathways than the former. Transport along these multiple pathways will have separate and distinctive travel times. In extreme cases, a significant portion of the tracer may be travelling along slow pathways and will not appear during the normal duration of an experiment. One key to testing this hypothesis may be to understand the detailed geometry of the conductors in the area of tracer test.

Another aspect of the multiple pathways is that multiple water sources will most likely be encountered. Most mathematical solutions to tracer transport only consider transport within a single planar feature. In three-dimensional networks, intersections, which appear along a tracer-transport pathway, may feed additional untraced water to the stream line/flow path, thus altering the flow field and diluting the tracer concentration.

2.4.3.4 Effects of retention processes

Recovery can be affected by retention processes. This issue is closely related to the effects of complicated flow paths discussed above. Matrix diffusion and reversible sorption should only retard transport, not stop it. Breakthrough curve forms should have some distinguishing characteristics, and there should be a dependency of the effect on velocities and pumping rates. This could be a particularly complicated hypothesis to test if it is combined with the effects of multiple complicated pathways, and especially if the pathways have different matrix interaction effects (mineralogy and chemistry) as well as different advective travel times (transmissivity and porosity).

2.5 Task 3.3.9.4 Channel Network 99.03 Model

During 1999, Golder developed and implemented a PAWorks channel network model for the TRUE-BS block based on the project hydro-structural model. Fracture networks represent a three-dimensional flow and transport regime made up of interconnected two-dimensional features (fractures). Channel networks are a method of reducing the complexity of flow and transport solutions within fracture systems to improve computational efficiency and the representation of channeling processes along fracture planes. They reduce flow and transport to a one-dimensional process along "stream tubes", which can significantly reduce processing time. A channel network model transforms a 3D discrete fracture network into a network of 1D pipes. Pipes are geometric connections between fracture traces formed by the intersection of two or more fractures (Dershowitz et al. 1998).

The pipes that make up the pathways within a channel network are, at the very basic level, derived from continuum streamlines defined by pressure contours. However, since both connectivity and flow in most fractured rocks are controlled by fractures, a smooth, continuous field of streamlines may not accurately define the flow field. A channel network takes these variations due to geometry into effect. Each fracture intersection is reduced from a line connecting two points to a single node. Channels, or "pipes", simply become lines connecting nodes. Pathways are composed of multiple pipes. Pipe properties, such as aperture, transmissivity, roughness and mineral infillings are either derived from the fractures themselves or are specified independently. Figure 2-9 illustrates the basic methodology behind the channel network approach.

A discrete fracture network (DFN) model is converted to channels through the use of the PAWorks software package (Dershowitz et. al., 1998) A 3-D network of fractures is first converted into a 1-D pipe network mesh. The finite-element code MAFIC is then used to calculate heads and fluxes at all nodes to produce a flow solution for the network. The PAWorks module analyzes transport pathways based on a search algorithm (Dershowitz et. al. 1998). Transport with PAWorks channel networks can be solved using the Laplace Transform Galerkin algorithm, which provides for advection and sorption onto the fracture surface, diffusion into the rock matrix and stagnant (non-flowing) water adjacent to the flowing fracture, and for radionuclide decay.

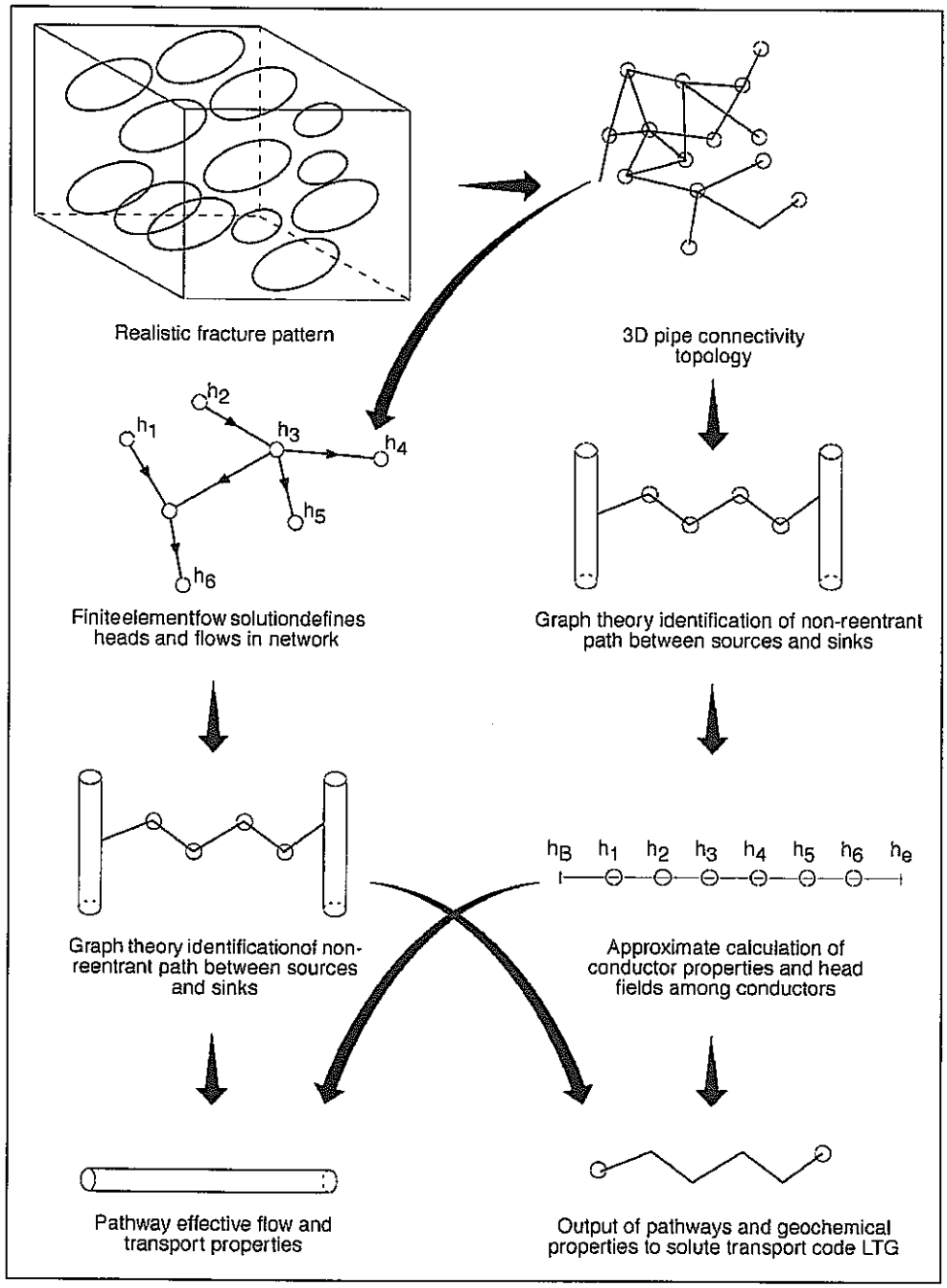

Figure 2-9 PAWorks Channel Network Pathways Approach

The PAWorks channel network model was based on a FracMan discrete fracture network (DFN) model containing 18,724 fractures, 18,699 of which are conditioned stochastic background fractures that reside in a 200m x 200m x 200m cube within the larger 500m x 500m x 500m scale structural model.

Fractures contained within the DFN model are converted to pipes based on the following assumptions:

- Effective Pipe Generation:

  Pipes cannot overlap each other. Pipes cannot cross fracture traces on a given fracture surface. In addition, to prevent excessively long pathways, additional pipes are added so that the tortuous distance between two nodes does not exceed the effective pipe factor times the Cartesian distance.

  Effective pipe factor = 2

- Pipe "Aperture":

  Pipe aperture is derived from fracture transmissivity using a power-law relationship: Aperture = $A*T^B$
  A=Aperture = 0.5, B=0.5, T = Transmissivity

  These parameters were derived from repeated experiments designed to simulate inflow into the TRUE boreholes.

- Pipe Width:

  The pipe flow width for a pathway is calculated based on the trace width of the fracture intersections forming the pipe. Pipe width is calculated using the following formula:

  $$\text{Width} = (X_{min} * L_{min}) + (X_{max} * L_{max})$$

  where L_{min} is the length of the shorter trace and L_{max} is the length of the longer trace. X_{min} and X_{max} are user-defined pipe width factors, which typically lie in the range of zero to one.
  $X_{min} = 1$, $X_{max} = 1$

  Figure 2-10 illustrates how pipe widths are calculated within the PAWorks code.

- Merge Distance = .001 m

  Any nodes that are closer together than .001m are merged together into one node. This has the effect of eliminating a fracture from the model.

- Minimum Transmissivity: $T = 1.00 \times 10^{-12}$ m^2/s

  Any pipes with transmissivities less than this value are eliminated from the CN model.

- External Model Boundaries:

  The external boundary of the preliminary CN model are the edges of the 500m x 500m x 500m cube of the September 1998 structural model. All external boundaries are modeled as constant head, and are set to the conditioned head field values presented by Holton (1999).

- Internal Boundaries:

  Two types of internal boundaries were used in the model: source zones and sink zones. Zones are described as the area between two packers (i.e. a "packer interval"). Sources were modeled as having a constant flux of zero. Sinks were modeled as constant flux, with a flow rate of 2.5833×10^{-5} m^3/s (1.55 l/min) during the simulation of interference test ESV-1a, and a flow rate of 1.333×10^{-5} m^3/s (0.8 l/min) during the simulation of interference test #1 (Andersson et al, 1998).

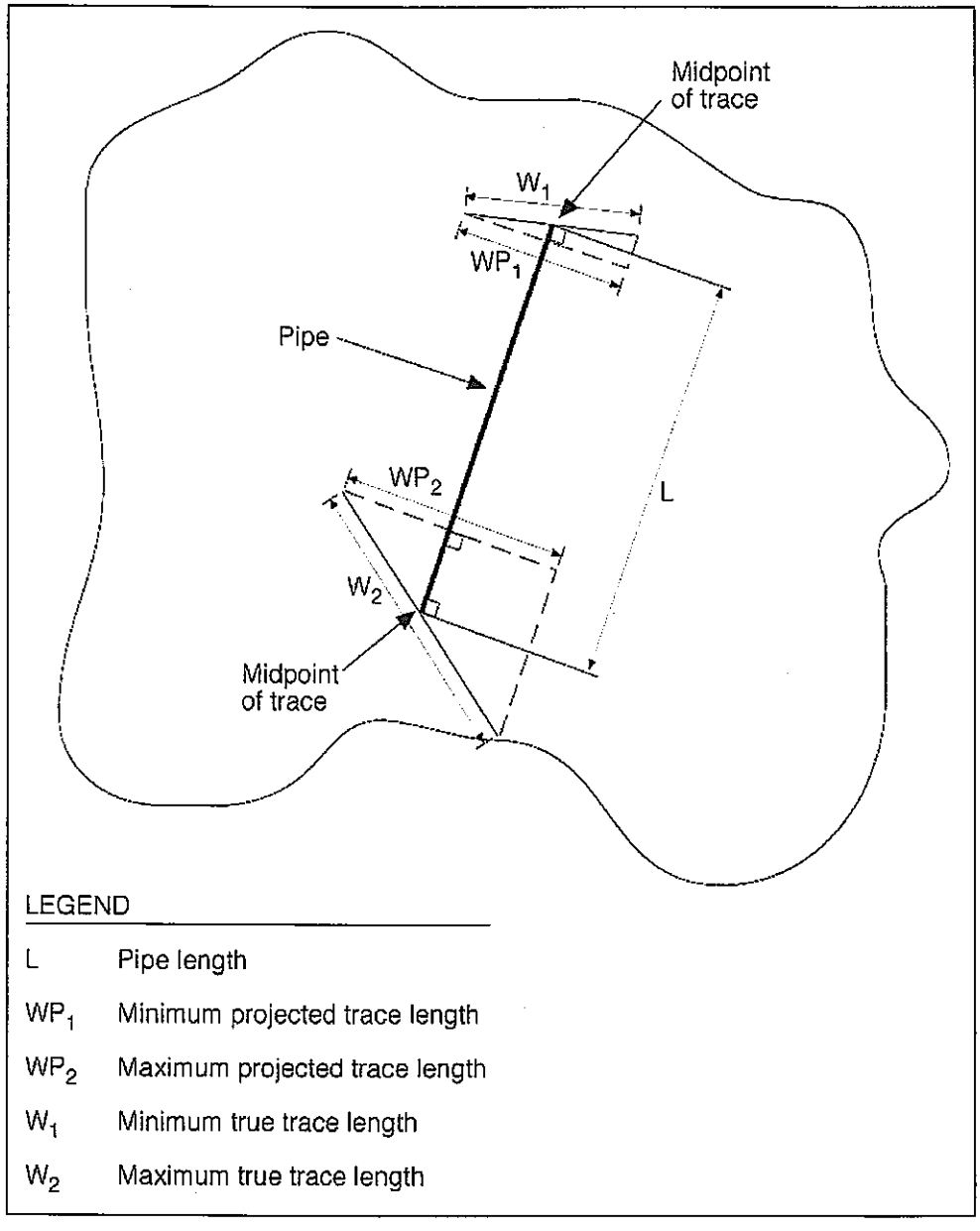

Figure 2-10 Algorithm for Pipe Width Calculation

2.6 Task 3.3.10.1 DFN Technical Review

Golder assisted the TRUE-Block Scale projects through participation in technical committee meetings which provided technical reviews of project structural and DFN modelling activities.

2.7 Task 3.3.11.2 Tracer Test Design/CN Task Modeling

In a fracture network, the area on a fracture where another fracture intersects has the potential of having either enhanced or reduced permeability and porosity when compared with the rest of the fracture. Depending on the effects that fracturing has on existing fractures the fracture intersection zone (FIZ) can be developed as a highly permeable flow channel or as a flow barrier. Alternatively, the result is a mixture of both, or the effects are minimal, making it distinction difficult from the heterogeneity in individual structures.

This task focused on PAWorks pathways analysis of Fracture Intersection Zone (FIZ) effects on Structure #20, which was the focus of tracer test design, together with hypothesized intersecting Type 2 Features #21 and #22. A plan view of Structure #20 depicting the geometry of these intersections is shown in Figure 2-11.

Structure #20 is currently intersected by four boreholes (KA2563A, KI0023B, KI0025F02, KI0025F). The locations of these intersections are shown in Figure 2-9. In addition to these existing intersections two additional hypothesized intersections (new_1 and new_2), representing new boreholes, were included in the model so that various well pairs for the tracer tests could be investigated.

It is assumed that Structure #20 contains a number of random flow channels. Their locations are not known. At the intersections of Features #21 and #22 with Structure #20 two FIZs are assumed, both of which form deterministic flow channels with known locations.

Channel network model

The channel network model for this study contains deterministic elements (Structure #20, Type 2 Features #21 and #22, and the packer intervals) as well as stochastic elements (the random flow channels). The model region is 120 x 120 m. Channels are located by a Poisson line process, with transmissivity according to a defined transmissivity distribution.

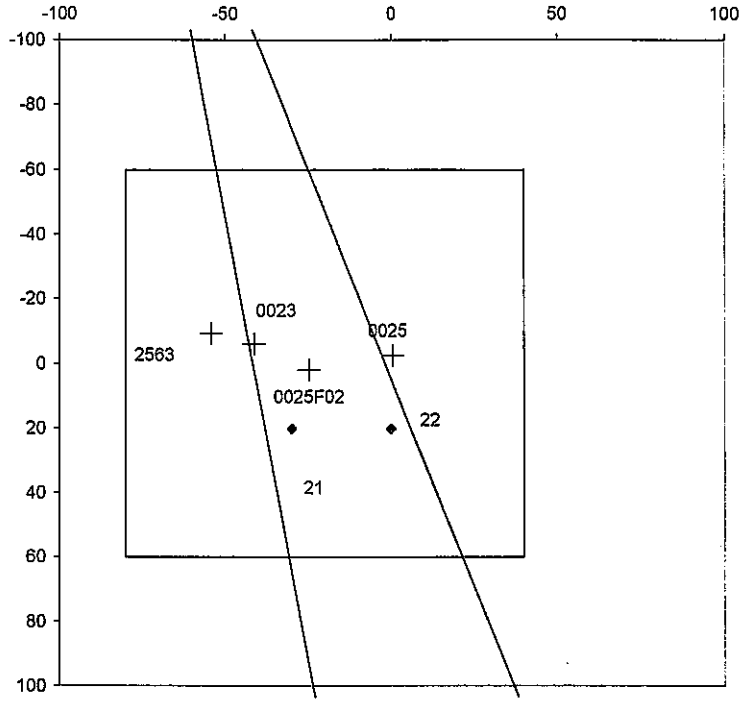

Figure 2-11 Intersections in the plane of Structure #20 with Type 2 Features #21 and #22 and existing and hypothesized new exploration boreholes

Five to twenty realisations of the channel network pattern were generated on each fracture plane. The locations and transmissivities of all channels except for the FIZ follow a Poisson line process. Transport apertures were calculated using the following equation: $e = 2 \cdot T^{1/2}$.

Simulation strategy

The tracer tests were simulated as radially converging tests. The model contains one sink zone, which is located in one of the new borehole locations. The sink zone is withdrawing water at a constant rate of 1 l/min. No active injection takes place at the source locations. The respective head field was calculated using MAFIC1D.

The previous generic model used a dipole test configuration. The dipole test is penetrating a larger region, so that effect of the FIZ was diluted. Radially converging tests typically affect smaller regions. Therefore it is hoped that a radially converging test gives a better resolution of the FIZ than what was seen in the generic FIZ model. To assess the effect of the FIZ the tracer breakthrough time was computed for the following three well pairs:

- Pair 1: KA2563A to new_1 (across the FIZ),
- Pair 2: KI0023B to new_1 (parallel to FIZ),

- Pair 3: KI0025F02 to new_1 (not affected by the FIZ), and
- Pair 4 : KI0025F to new_2 (across FIZ).

Tracer is added at the respective borehole locations by dilution. Tracer breakthrough at the sink locations was calculated using PAWorks/CTG (Dershowitz et al., 1998).

Transmissivity models

The 'visibility' of the FIZ will largely depend on the transmissivity in the FIZ and in the surrounding flow channel network. To study this aspect these three different pipe network cases were generated:

- Case 1: Homogeneous pipe network, where all pipes including the FIZ have the same transmissivity ($1 \cdot 10^{-6}$ m^2/s),
- Case 2: Homogeneous pipe network with increased transmissivity for the FIZ ($1 \cdot 10^{-4}$ m^2/s), and
- Case 3 and 4: Heterogeneous pipe network, where the pipe transmissivities are random (Normal of Log distribution) except for the FIZ, transmissivity for the FIZ equals mean of transmissivity distribution ($1 \cdot 10^{-6}$ m^2/s).

Cases 1 and 2 assume a homogeneous flow channel network. In Case 1, it is also assumed that the FIZ has no increased transmissivity compared to the flow channels in other areas of the fracture. In Case 2 the FIZ transmissivity is increased in comparison with the transmissivity of the flow channels.

For Case 3 it is assumed that the transmissivity along the flow channels varies significantly (Normal of Log distribution with standard deviation of one order of magnitude). For Case 4, the standard deviation is four orders of magnitude in the flow channels. The FIZ has no increased transmissivity, i.e. its transmissivity equals the mean of the Normal of Log distribution. These cases are used to study whether it is possible to distinguish between a homogeneous flow channel network with an FIZ and a heterogeneous network without an FIZ.

Results

Breakthrough curves were generated and the median breakthrough time was calculated (t_{50}) for the four cases and for four different well pairs, cf. Table 2-3. An example suite of breakthrough curves is shown in Figure 2-12.

	Median Breakthrough Time T_{50}, (hours)			
Source interval	KI2563	KI0023	KI0025F02	KI0025
Sink interval	new_1	new_1	new_1	new_2
Case 1: Homogeneous	80.52	52.36	27.77	27.01
Case 2: Homogeneous with increased T for FIZ	161.51	94.29	27.14	53.86
Case 3: Heterogeneous with Std. Dev. = 1 order of mag.	94.28	58.28	31.91	17.35
Case 4: Heterogeneous with Std. Dev. = 4 orders of mag.	485.95	190.10	93.59	75.65

Table 2-3 Calculated median breakthrough time t_{50} for the hypothesized new sink sections in New_1 and New_2

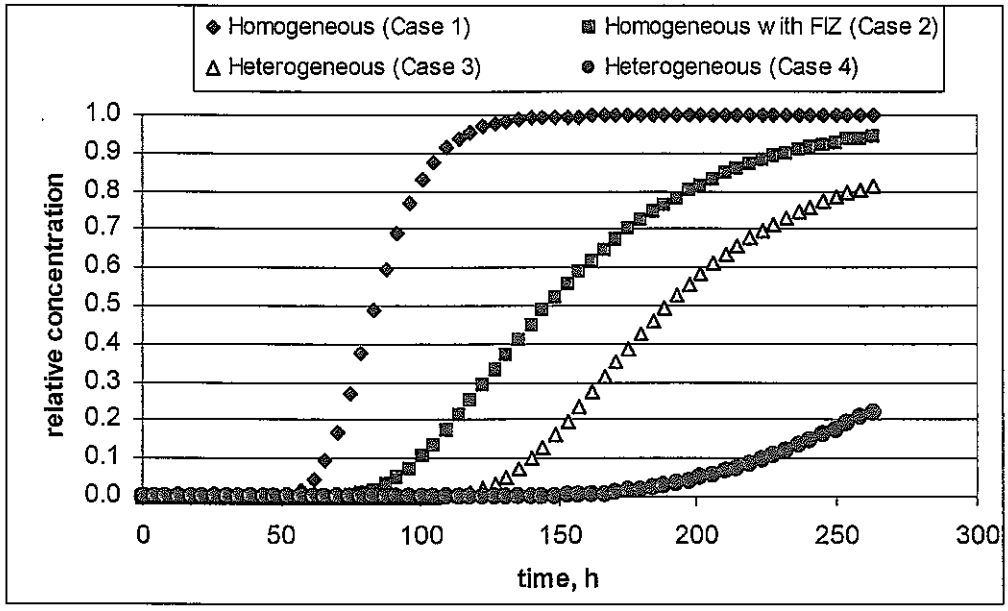

Figure 2-12 Example suite of breakthrough times for injection in KA2563A and pumping in New_1.

It can be seen in Table 2-3 that for the source intervals KA2563A and KI0023B an increased transmissivity in the FIZ causes a doubling of the breakthrough time. This is caused by the larger fracture aperture that is assumed in the model for fractures with an increased transmissivity. The larger aperture causes a slower flow velocity and thus, a longer travel time.

Surprisingly, tracer released in KI0023 is affected as much by the FIZ as tracer released in KA2563A although tracer does not have to travel directly through the FIZ. Obviously the FIZ changes the overall flow field and changes the flow velocity in the flow channels in its vicinity.

As expected, tracer released at source interval KI0025F02 is not effected by the FIZ. Hence, the breakthrough times for Cases 1 and 2 are identical.

For a heterogeneous channel network, the effects of the varying transmissivities show in the large range of breakthrough times for the different realisations. For tracer released in zone KI0025F02 for example the breakthrough times range from 18.5 hours to 494 hours. Overall, the existence of slower sections in the pathway causes most realisations to have longer breakthrough times. Hence, the median breakthrough times for Case 3 are approximately twice as large as the median breakthrough times for Case 2.

Identification of FIZ in a field situation

In reality, if the existence of an FIZ is to be investigated, it is obviously not possible to compare test results for cases with and without an increased transmissivity in the FIZ. Instead only one of the cases discussed above, or a combination of them exits, and the goal is to unveil the actual situation. A comparison of possible test results can only be made for the three different well pairs.

As shown before, the velocity for tracer released in zones KA2563A and KI0023B should be affected, if a higher transmissivity exists within the FIZ. In opposition to that, the velocity for tracer released in zone KI0025F02 should not be effected. Hence, a comparison of the tracer velocities should reveal the existence of an FIZ.

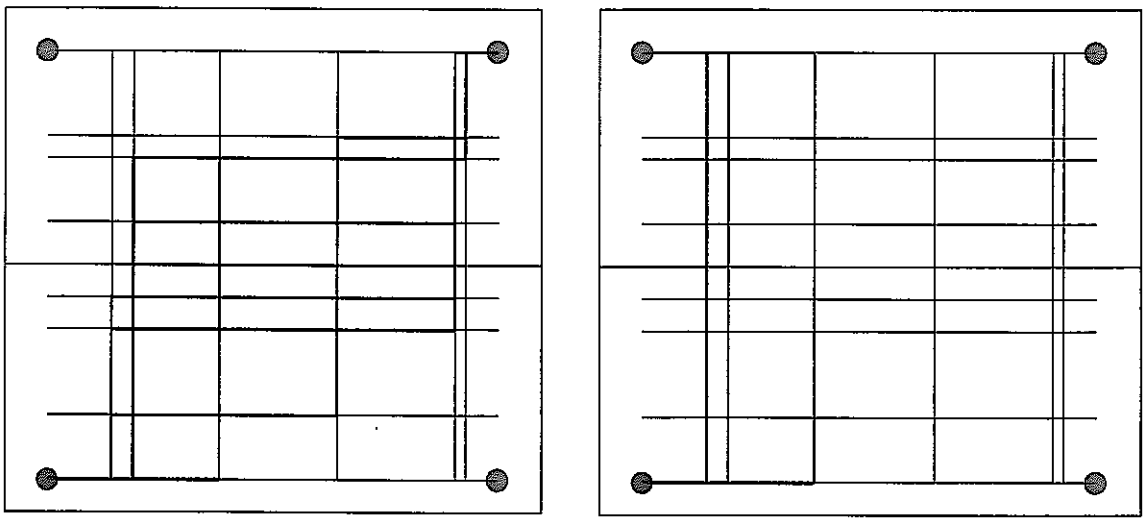

Figure 2-13 Area affected by diagonal and perpendicular well pairs, respectively

However, as shown in the generic FIZ model, the tracer velocity will also be effected by the pipe network geometry. Generally, flow velocity is a function of the flow rate and the flow cross sectional area. In this case the area is the sum of the single pipe cross-sectional areas weighted by flow fraction.

In the previous model in the case of the diagonal well pair the cross sectional area was significantly larger than in the case of the perpendicular well pair, cf. Figure 2-13. Hence, the flow velocities for the diagonal well pair were always slower than for the perpendicular well pair.

In order to eliminate this effect the test configuration was changed to a radially converging flow, where mainly a series of flow channels or different geometry are affected, rather than a set of channels parallel to the flow direction. Furthermore the well pairs are all similarly oriented compared to the pipe network (diagonal flow pattern). Therefore all well pairs should be effected in a similar way.

2.8 Task 3.3.12.1 CN Modelling of Pre-tests

Under this task, Golder implemented a FracMan/PAWorks channel network (CN) model for tracer pre-tests PT-1 through PT-4. The model incorporated the latest Aspo HRL structural model revision (Hermanson, 1999) with a conditioned background fracture model (Fox, 1999).

Tracer tests PT-1 through PT-4 were conducted as part of the TRUE Block Scale Detailed Characterization Stage, as a way of selecting pathways and conductors for later, larger-scale tests. PT-1, PT-2 and PT-3 were performed as tracer dilution tests under both natural flow and pumping conditions. PT-4 was performed as an injection tracer test in a system with radially converging flow geometries (Andersson, 1999).

2.8.1 Model and Test Parameters

Pre-tests 1 through 4 were modeled utilizing the latest Aspo HRL structural model revision, which adds two new fractures (21 and 22) to allow for pathways connecting Structures 13 and 20. A set of conditionally generated background fractures were added to provide for additional connectivity within the TRUE Block [Fox, 1999]. Table 2-4presents a summary of the model, while Figure 2-14 illustrates the current structural model in 3-D. Figure 2-15 is a tracemap view of the March 1999 Structural model at the center of the block (Z = -450 m).

A fracture transmissivity distribution for background fracturing is derived from flow logging results in the TRUE Block boreholes (Gentzschein, Jan. 1997; July 1997; Feb. 1998). Results from the 5m dual-packer logs are entered into the Oxfilet module of FracMan, which then calculates transmissivity distributions (Dershowitz et al, 1998). Background fracture intensity was derived from both the September 1998 structural model A procedure for estimating P_{32} from P_{10} is described in TN 97-32b (Follin, Wei 1997).

large-scale Features	27 fractures: (22 Primary fractures, 5 bounding faults) March 1999 Aspo Structural Model (Hermanson, 1999)	
Background Fractures	Derived from drill logs, BHTV, POSIVA flow logs and borehole radar measurements in the following TRUE Block Scale boreholes (KA2511A, KA3510A, KA2563A, KI0025F, KI0023B, KA3573A, KA3600F, KI0025F02)	
	Fracture Model	Enhanced Baecher
	Orientation Model	Bootstrap: Dispersion (K) = 200
	Size Model	LogNormal distribution Mean = 6 m Std Deviation = 2 (after Hermanson et al, 1997)
	Termination %	25
	Intensity (P32c)	0.293232 m^{-1}
	Transmissivity Distribution: Truncated LogNormal	Mean (arithmetic) : 10^{-7} m^2/s Std. Dev. (arithmetic) : $8*10^{-6}$ m^2/s Max:1 m^2/s Min: 10^{-10} m^2/s
	# of Fractures	18,699

Table 2-4 Current Structural Model

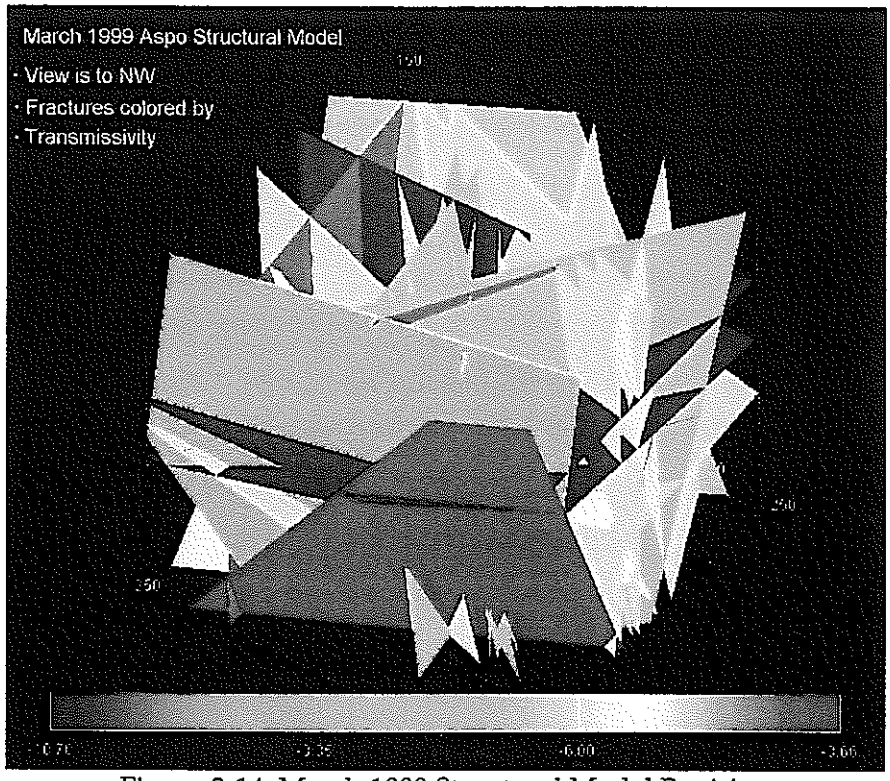

Figure 2-14 March 1999 Structural Model Revision

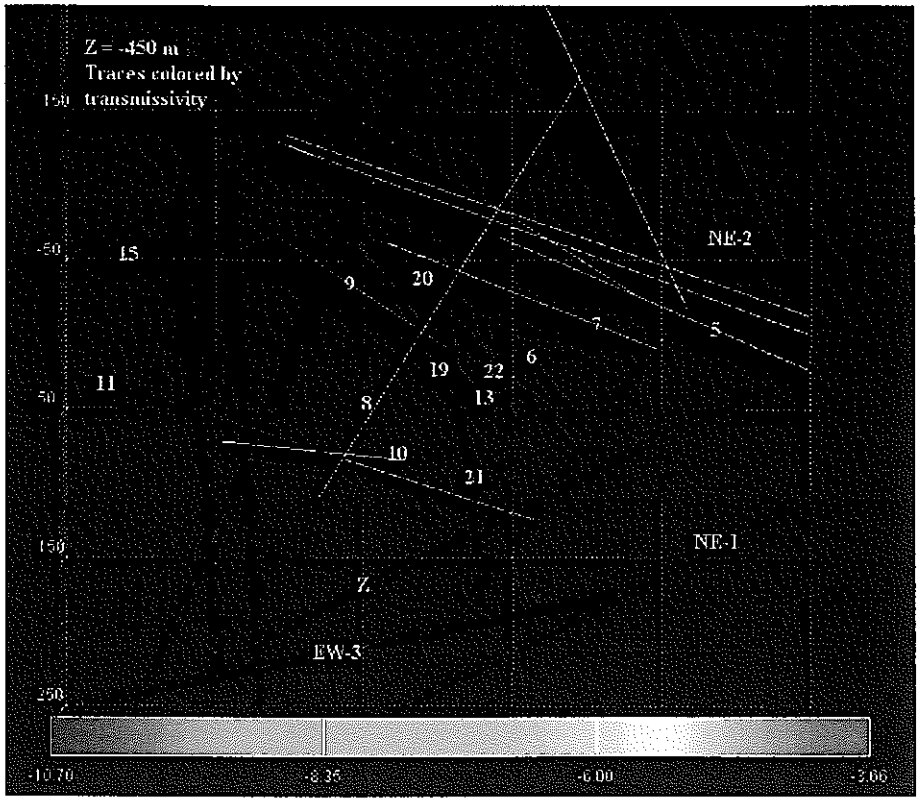

Figure 2-15 March 1999 Structural Model: Trace map View

Structure 9 was left in the model, even though its significance as a conductor has since been eliminated doubt at the time. A 500 m x 500 m x 500 m cube was modeled, with background fracturing present only within an inner 200m x 200m x 200m block.

Table 2-5 presents the scopes and objectives of the pre-tests (Andersson, 1999).

Test #	Objective	Implementation
PT-1	Test connectivity within Structure #13 and between #13 and #20	Tracer dilution test, with sink in KI0023B:P4 (Structure #13) (84.75 m – 86.20 m)
PT-2	Test connectivity within #20 and between #20 and #21, #22, #13 and #6	Tracer dilution test, with sink in KI0023B: P6 (Structure #21) (70.95 m - 71.95 m)
PT-3	Test connectivity within #20 and between #20 and #21, #22, #13 and #6	Tracer dilution test, with sink in KI0025F02: P5 (Structure #20) (73.3 m – 77.25 m)
PT-4	Test transport connectivity and assess transport properties	Radially-converging tracer injection test, with sources and sinks determined by PT-1 through PT-3

Table 2-5 Pre-Tests Scope and Objectives

All simulations were run using a set of external boundary conditions provided by AEA Technology [Holton, 1999]. Freshwater heads were used at all external boundaries, with no corrections for density or salinity. Simulations were run only for the specified duration of the test. Table 2-6 presents the specific testing parameters used. PT-1 through PT-3 were run as transient flow simulations, while PT-4 was run solely as a steady-state simulation.

Parameter	Values
PT-1	
Pumping Rates (minutes | l/min)	+ .001 min : 0.89 l/min + 50 min : 0.75 l/min +100 min : 0.7125 l/min +200 min : 0.695 l/min +400 min : 0.6875 l/min +1440 min : 0.68 l/min
Output Times	Same as pumping times
Test Duration	24 hours (1440 min)
PT-2	
Pumping Rates	+.001 min : 2.85 l/min +100 min : 2.75 l/min +275 min : 2.75 l/min +1250 min : 2.6 l/min +2000 min : 2.575 l/min +2700 min : 2.55 l/min +2880 min : 2.55 l/min
Output Times	Same as pumping times
Test Duration	48 hours (2880 min)
PT-3	
Pumping Rates	+0.0001 min : 4.8 l/min +2880 min : 4.8 l/min
Output Times (min)	.001, 166.67, 416.67, 1250, 2500, 2880, 2881
Test Duration	48 hours (2880 minutes)
PT-4	
Injection Rate	Constant Flow KA2563A: S4 -- 600 ml/hr KA2563A: S1 -- 400 ml/hr KI0025F02: S3 -- 140 ml/hr KI0025F02: S6 -- 460 ml/hr
Injection Duration	KA2563A: S4 --- 213.92 KA2563A: S1 --- 476.5 hrs KI0025F02: S3 --- 192.75 hrs KI0025F02: S6 --- 212.75 hrs
Test Duration (how long observations were taken)	KA2563A: S4 --- 401.0 hrs KA2563A: S1 --- 750.0 hrs KI0025F02: S3 --- 401 hrs KI0025F02: S6 --- 401.0 hrs
Pumping Rates	KI0023B: P6 Constant Flow: 2.5 l/min

Table 2-6 Pre-Test Simulation Parameters

For PT-4, an ideal conservative tracer was used, with $K_d = 0$, free-water diffusivity = 0.032, and $\mu = 9.39 \times 10^{-15}$. The tests were simulated as four different dipole tracer tests in a steady-state system.

PT-1 through PT-3 were simulated as simple drawdown tests, with heads and head drops at individual borehole segments as output. Figure 3-1 shows the finite-element mesh, with individual pipes colored by transmissivity.

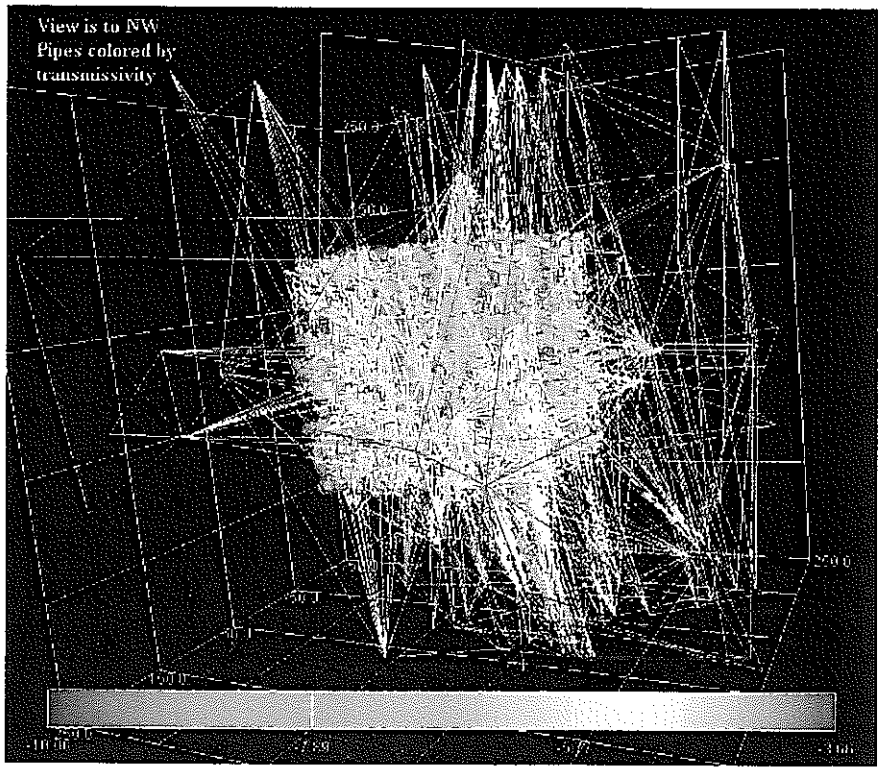

Figure 2-16 CN model of Aspo TRUE Block site

The test results were then loaded into an Excel spreadsheet, where distance-drawdown plots were completed. These graphs plot absolute drawdown for the entire test (in kilopascals) versus time divided by distance squared (T/R^2). Distances are from packer interval midpoints. All points were plotted assuming the late-time breakthrough value used in the hydraulic analysis of PT1 through PT3 (Doe, in prep).

Figure 2-15 shows a sample distance-drawdown plot, while Figure 3-3 shows the comparison plot from the hydraulic analysis of the pre-test series.

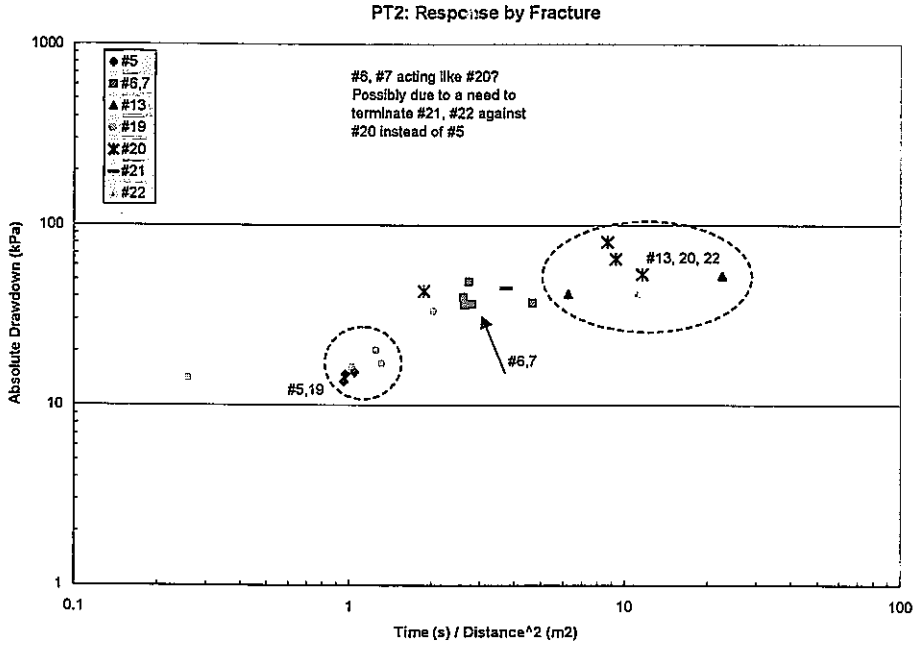

Figure 2-17 Simulated Distance-Drawdown Plot

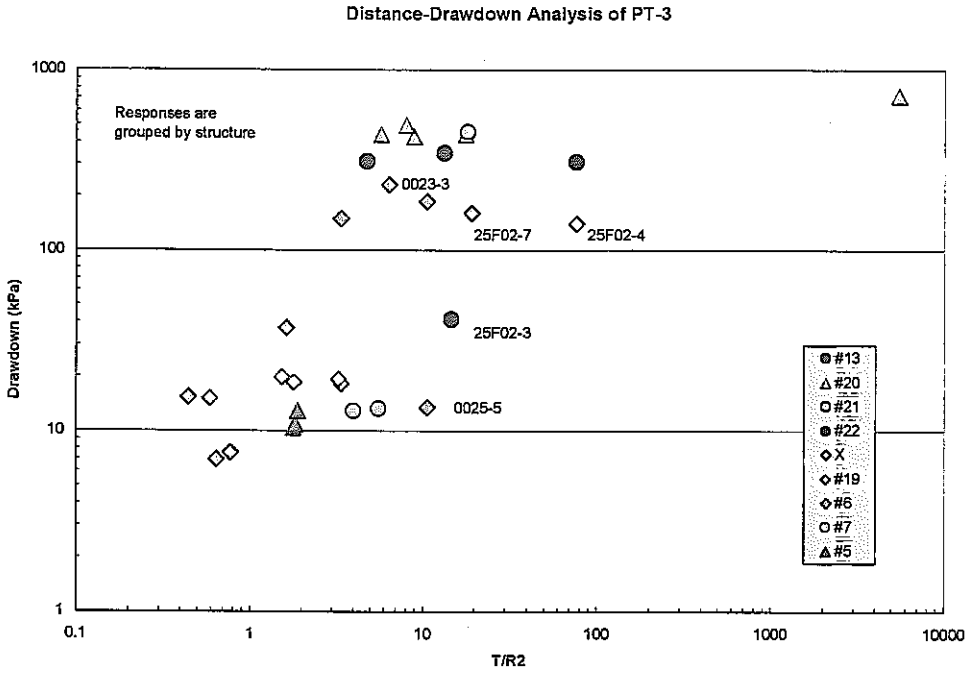

Figure 2-18 Distance-Drawdown plot based on actual Pre-Test data

In general, pre-test simulations agreed qualitatively with the analysis of the actual test data. However, there are several discrepencies, which are addresses in subsequent modeling

2.9 Task 3.3.13 Modelling Workshop

The TRUE-Block scale project held a modelling working during September, 1999 in Stockholm Golder prepared materials and presentations regarding the JNC modelling software and approaches for the TRUE-BS project (FracMan, MAFIC, PAWorks, FracDim, and LTG). Golder participated in this workshop, and ensured technology transfer from workshop participants to JNC.

2.10 Task 4.2.3 Geometrical Analysis

Golder assisted in analyses for borehole optimization for the tracer testing stage (TTS). Figure 2-19 illustrates the geometrical analysis which formed the basis for borehole-optimization analysis.

2.11 Task 4.2.11 Structural Model Update

This report describes a program of hydraulic data analyses to verify the March 1999 structural model (Hermanson, 1999) of the TRUE Block Scale experimental site. The analyses take advantage of information provided by the most recent borehole, KI0025F02 as well as the results of a program of pressure interference tests and tracer dilution tests that Geosigma AB performed to provide data to help design the main tracer testing phase for the TRUE Block Scale program (the Pre-Test or PT program, Andersson et al., 1999)).

The major objectives of this work are the following:

- Verification of March'99 structural model.
- Suggestions of revisions to structural model based on inconsistencies of the model and the hydraulic data.
- Production of an overlay to the March '99 model where the hydraulic significance of the structures is highlighted.
- Tabulation of transmissivities associated with the significant structures.

The structural model of the TRUE-block scale site has continuously evolved with the drilling, testing, and exploration of the True Block Scale volume. By the time the most recent borehole, KI0025F02, was drilled, the major geologic and hydrologic structures of the block were known with sufficient confidence to allow accurate predictions of the locations and relative hydraulic significance of these major structures. The major hydraulic structures of the site consist of several northwest trending fractures and fracture zones. These hydraulically significant zones

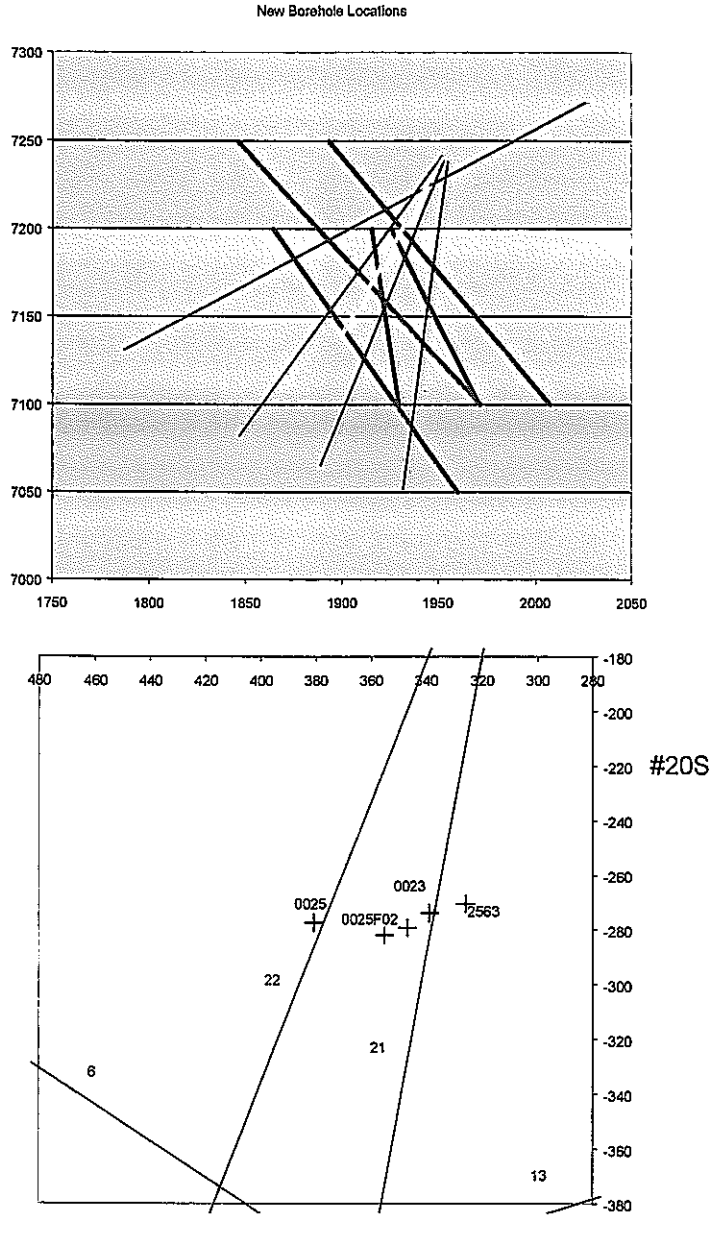

Figure 2-19 Example Analysis of Alternative Borehole Locations

are a subset of a larger family of geologically identified structures. Prior to the development of the March'99 model these structures were identified, in order of appearance from the borehole collars, as #5, #7, #6, #20, #13, #19, and #10. The location of these structures is shown in map view in Figure 2-17. Structures #5, #6,and #7 were sufficiently transmissive to require grouting to assure borehole stability, and were thus not considered as targets for the main phase of tracer testing.

The main goal of the TRUE-block scale program has been the testing of networks of features rather than single features, which was the focus of another phase of the TRUE program. Structures 19 and 10 were too isolated to form a significant fracture network. Hence the focus of the tracer-testing program moved to the major structures of the central portion of the True Block Scale volume, specifically Structures #20, #13, and #6. Structures #20 and #13 are sub-parallel, but were known from inference tests to be connected by conducting fractures that were not prominent enough to have been assigned numbers. A major goal of geologic analyses after the completion of KI0025F02 was to identify in more detail the fractures that connect these numbered structures. Based on analyses of the flow logs and geologic logs, two possible structures were proposed, which had more northerly trends than #13 and #20. These potential cross-cutting structures were given the designations #21, and #22 (Figure 2-20). Each of these structures was proposed on the basis of only two intersections, and there were no hydraulic interference data to corroborate their existence as conductive structures. Hence, one goal of the Pre-test program was to provide hydraulic data to test the March'99 additions to the structural model.

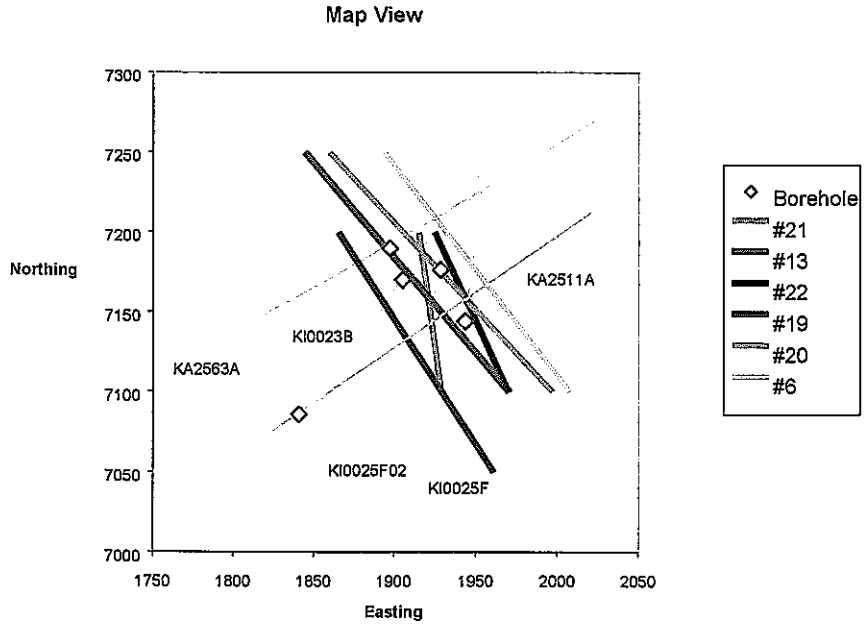

Figure 2-20 Map view of conducting structures in March '99 structural model.

Diamonds show intercepts of the boreholes with a horizontal plane at Depth= -480 meters. Please note, this map view shows the relative locations of the structures and takes no account of terminations.

2.12 Task 4.5.2 CN Prediction for Phase A

Golder assisted JNC in simulations to predict solute transport for the "Phase A" of the tracer testing stage (TTS). These simulations were carried out using the FracMan/PAWorks Channel Network (CN) model. The CN Prediction for Phase A included extensive calibration simulations

for tests A-1, A-2, A-3, and A-4 of Phase A, and a prediction for tracer breakthrough in test A-5. Figure 2-21 presents the injection time history for sorbing and non-sorbing tracers in tests A-5.

PAWorks channel network prediction simulation results are provided in Figure 2-22 through Figure 2-24. Figure 2-22 illustrates the distance drawdown response during the experiment. Figure 2-23 shows the head distribution in the model region during the test. Figure 2-24 shows the breakthrough curve predictions. Breakthrough statistics are summarized in Table 2-7.

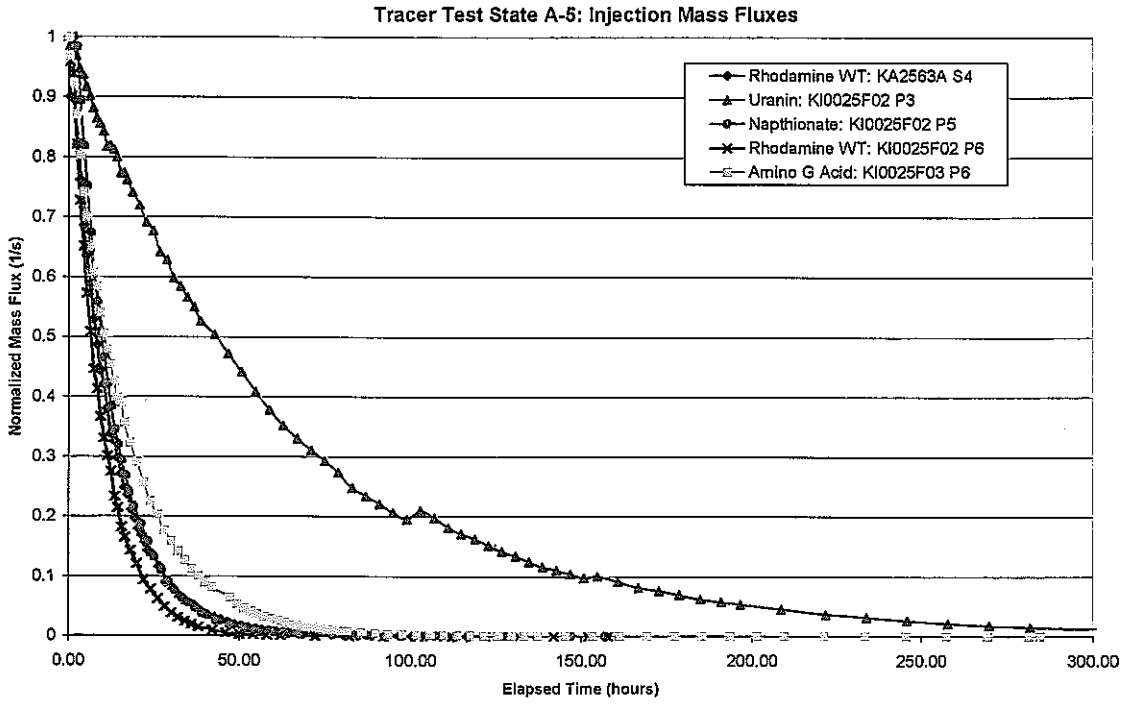

Figure 2-21 Injection Time History for Phase A-5 Tracer Test

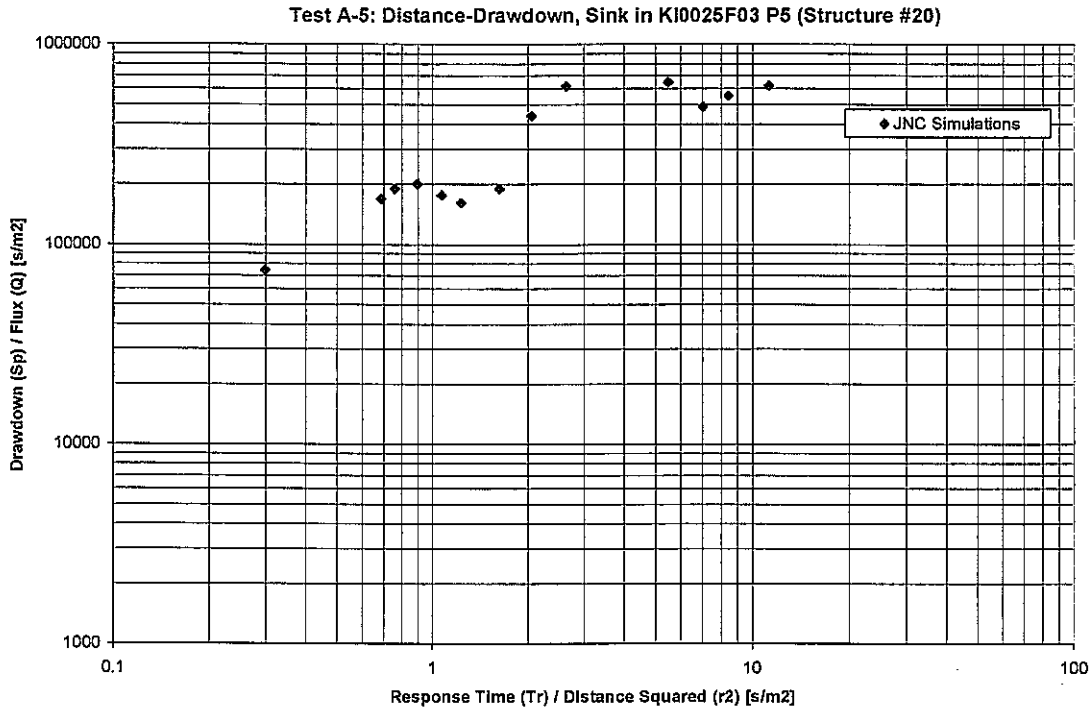

Figure 2-22 Distance Drawdown for Phase A-5 Tracer Test

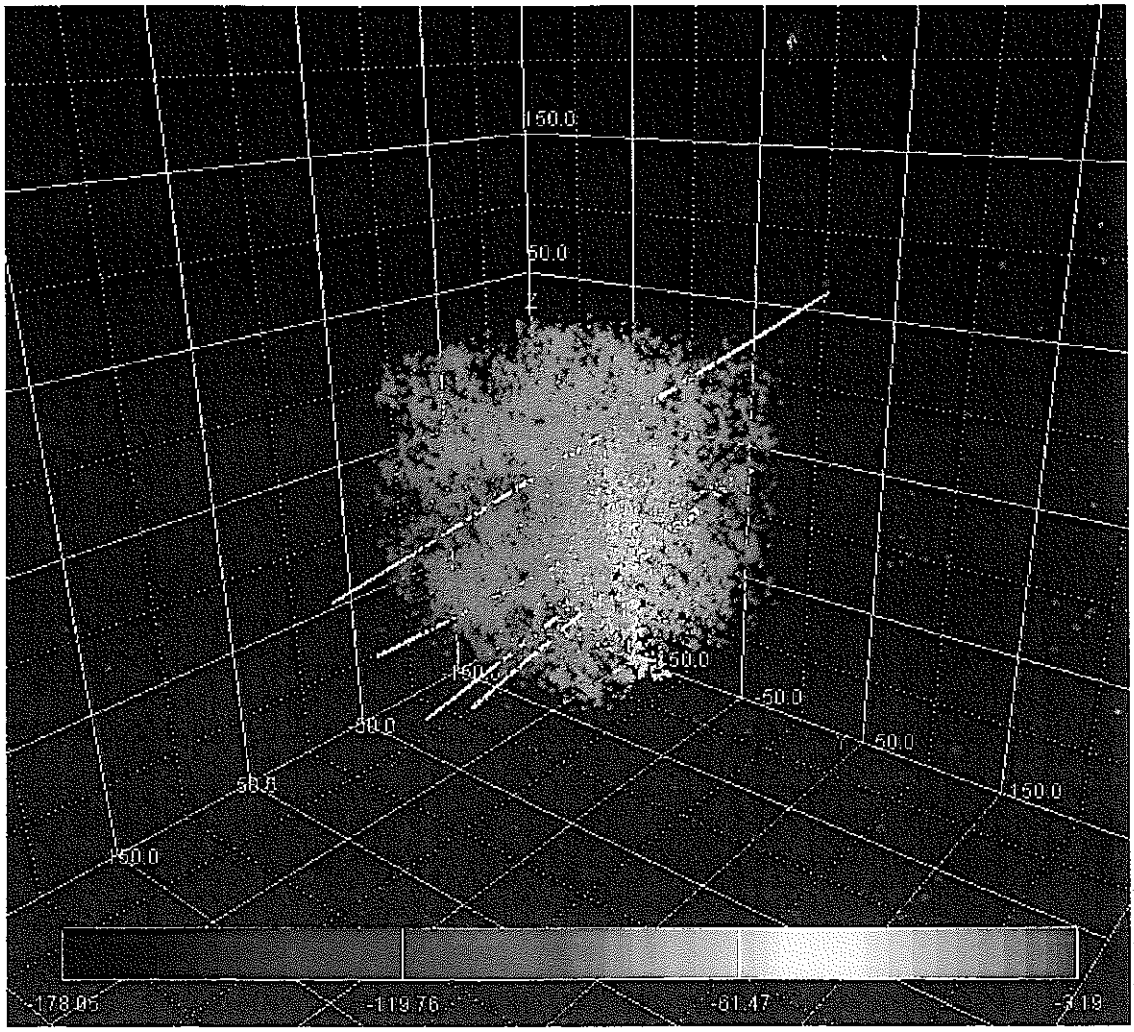

Figure 2-23 Head Distribution for Phase A-5 Tracer Test

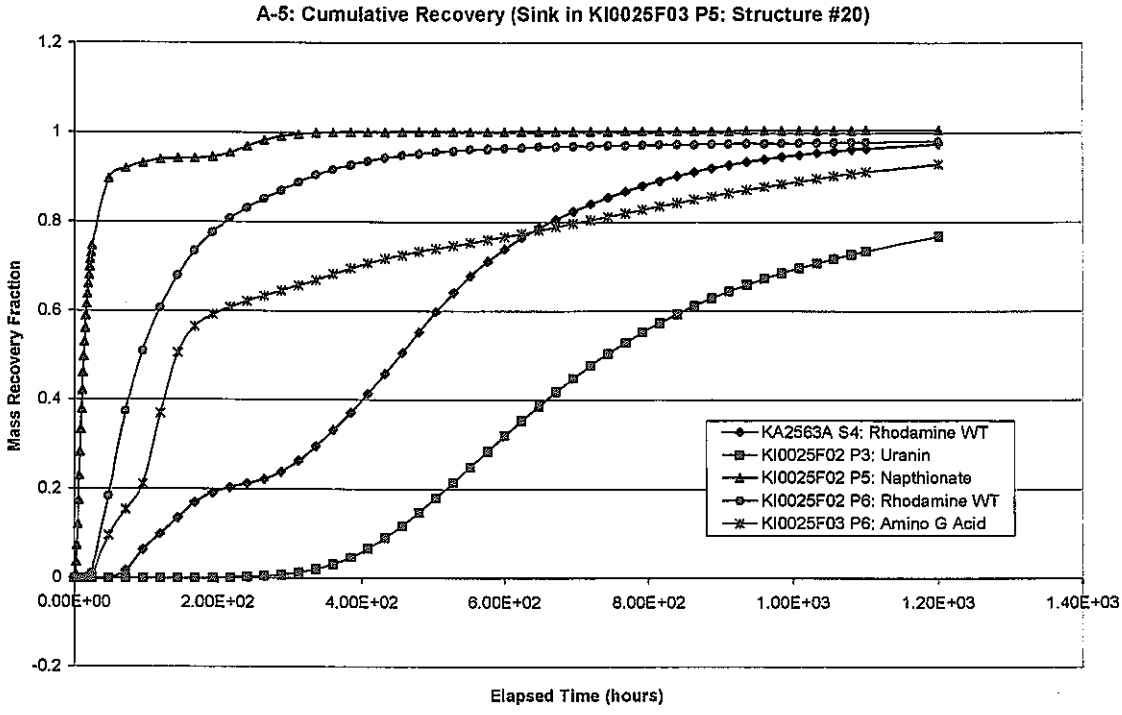

Figure 2-24 Phase A-5 Tracer Breakthrough Predictions

Species	T5 (hrs)	T50 (hrs)	T95 (hrs)
Rhodamine WT (1)	94	456	1008
Uranin	384	744	*
Napthionate	3.5	13	216
Rhodamine WT (2)	?	96	480
Amino G Acid	36	144	*

Table 2-7 Phase A-5 Predictions

2.13 Task 4.5.4 Compilation and Analysis of Background Fracturing

In this task, Golder carried out a statistical analysis of background fracturing from Posiva flow logs to develop an updated background fracture model to support tracer test modelling. The purpose of this study is to provide a quantitative basis for modeling of background fracturing in the immediate vicinity of the region where TRUE-Block Scale boreholes intersect Features #13,

#20, #21, and #22. This "TTS Region" and the features in it are the focus of the Tracer Test Stage (TTS) of the TRUE-Block Scale experiment (Figure 2-25).

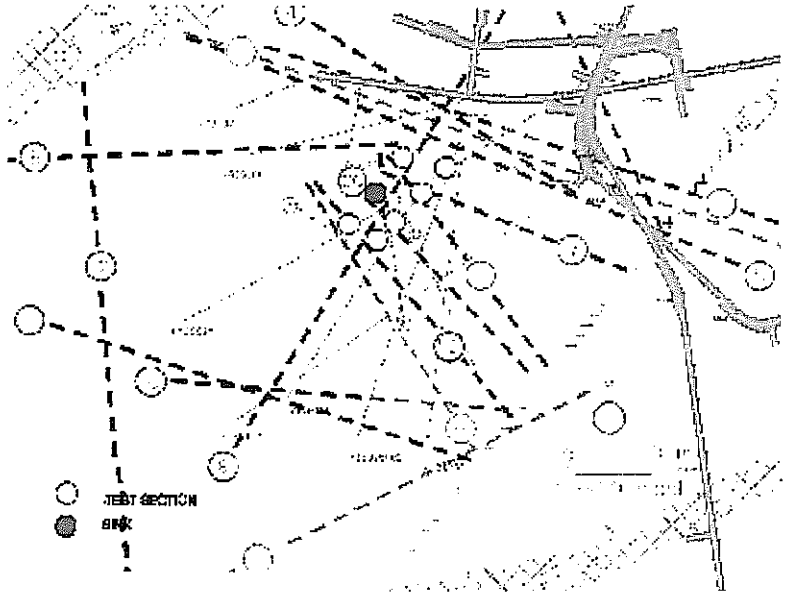

Figure 2-25 Tracer Test Region

JNC carried out analyses of fracture spatial structure, orientation, intensity, and transmissivity during 1999. This analysis was carried out based on features identified in Posiva flow logs. These features are illustrated in Figure 2-26. Figure 2-27 and Figure 2-28 present examples of transmissivity and spatial structure analyses carried out by JNC on TTS region Posiva Flow Log feature data during 1999.

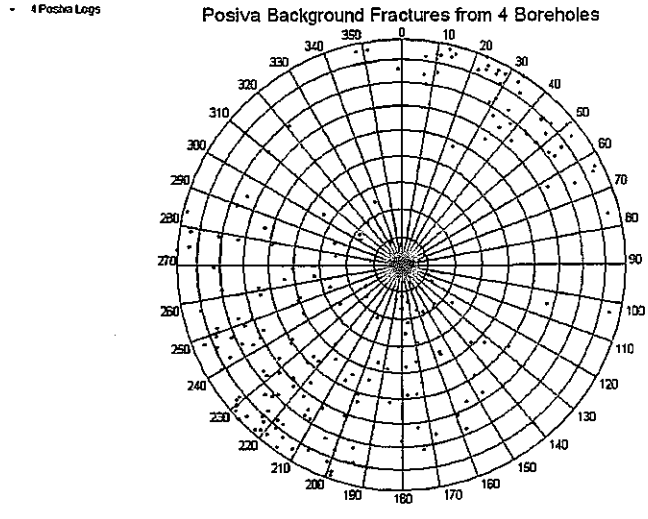

Figure 2-26 Posiva Background Fractures from TTS Boreholes

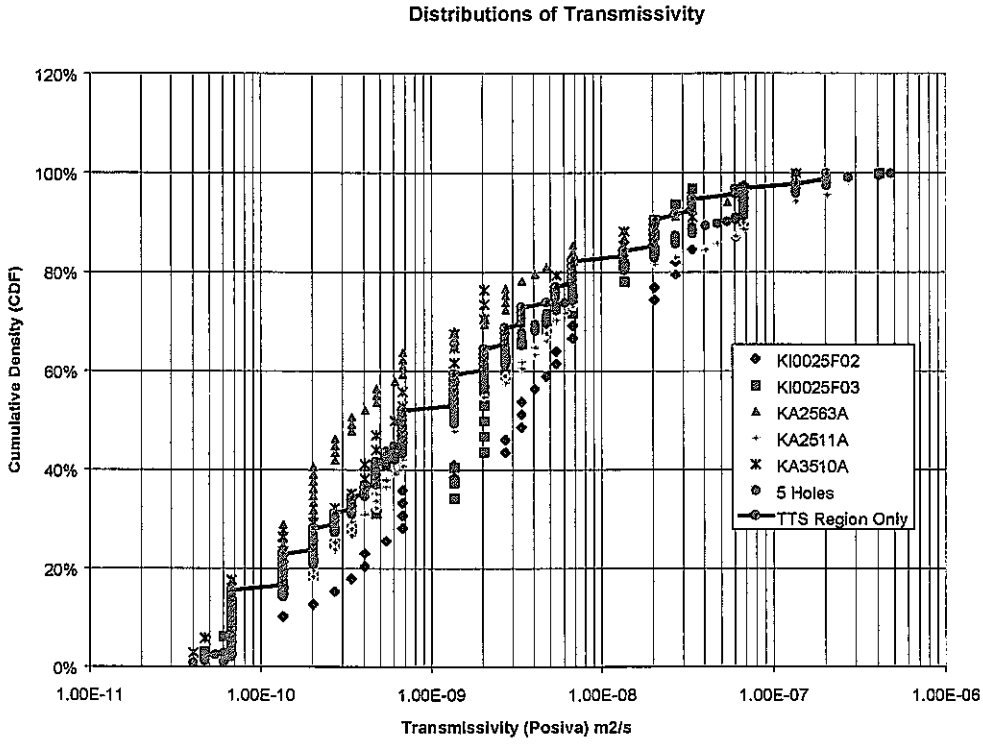

Figure 2-27 Transmissivity Distributions of Posiva Features

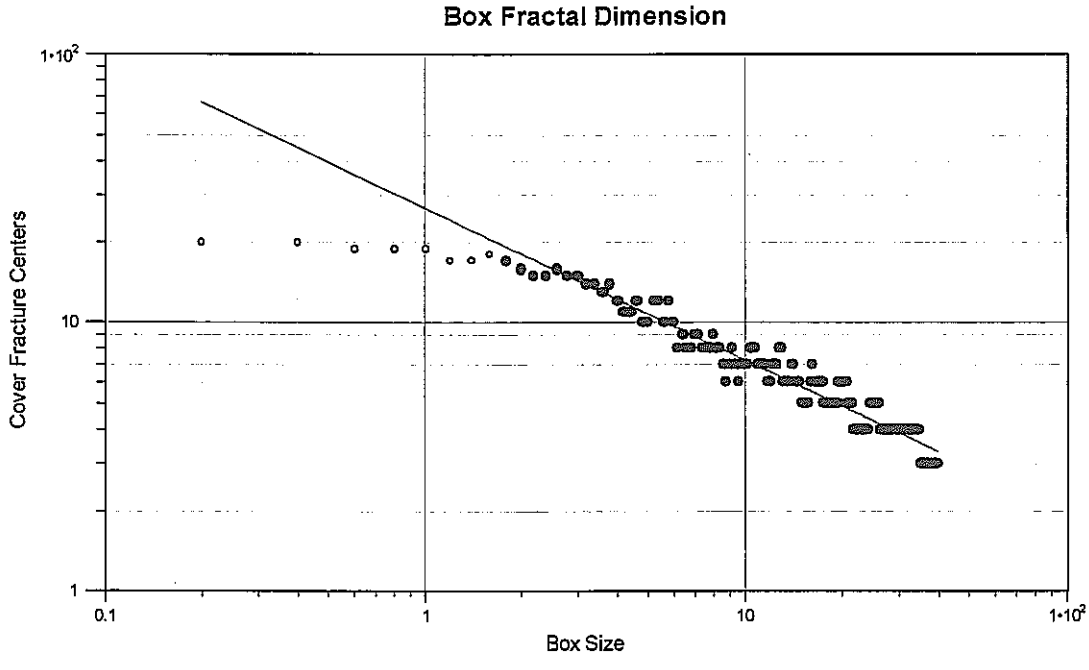

Figure 2-28 Example Spatial Analysis of Background Fractures

2.14 Task 4.5.5 Virtual Packer Location

Golder identifies the "virtual" packer locations which are consistent with both packers as installed and the feature locations as implemented in the structural model. These packer locations are summarized in Table 2-8.

Corrected Packer Locations and Interval Segments

Blue indicates changes; Gray shading indicates unmonitored intervals; Question marks indicate that the structure extrapolates to the interval, but the hydraulic evidence for it is uncertain or not existent.

KI0025F03	P-setting	Collar		Pkr10		#7		Pkr9		#6		Pkr8		Pkr7		#22		Pkr6		#20		Pkr5				Pkr4		#21			
		0		2.6	3.58	42.18	49.00	50.00		50.3	54.08	55.08		58.58	59.58	60.93	65.58	66.58		73.68	74.08	75.08				80.00	81.00	82.07			
KI0025F02	P-setting	Collar		Pkr10		Pkr9		#7		Pkr8		#6		Pkr7		Pkr6		#22		Pkr5		#20		Pkr4				Pkr3			
		0		2.4	3.4	37.5	38.5	42.57		50.7	51.7	53.32		55.1	56.1	63	64	67.07		72.3	73.3	77.25	77.5	78.5		92.35	93.35				
KI0023B	P-setting	Collar		Pkr9		Pkr8		#7		Pkr7		#6		#20		Pkr6		#21		Pkr5		Pkr4		#13		Pkr3		Pk			
		0		3.6	4.6	40.45	41.45	41.81		42.45	43.45	45.8		69.33	69.95	70.5	70.66	71.95		72.95	83.75	84.75	85.79	86.2		87.2	110.3				
	P-setting	Collar		Pkr7		Pkr6		Pkr5		Pkr4		#7		#6		#22?		#21?		Pkr3		#20		Pkr2		#13		#19		Pk	
		0		5	6	75	76	112		113	145	146		153.7	158.6	172.64	182.33	186		187	189.90	196	197	208.01		239.60	265				
KA2563A	R-setting	Collar		Pkr8		Pkr7		#7		#6		#22?		#21?		Pkr6		#20		Pkr5		#13		Pkr4		Pkr3		Pkr2			
		0		75	76	145	146	153.7		158.6	172.64	182.33		186	187	189.90	190	191		208.01	219	220	224	225		228.0	229				
	S-setting	Collar		Pkr8		#7		#6		#22?		#21?		Pkr7		#20		Pkr6				Pkr5		#13		Pkr4		Pkr3			
		0		146	146	153.7		158.6	172.64	182.33		186	187	189.90		190	191			205	206	208.01	209	210		235.00	236				
	P-Setting	Collar	Pkr7		#7		Pkr6		#6		Pkr5		#20		#22		Pkr4		#13		Pkr3		Pkr2		#19		#21		Pkr1		
		0	2.5	3.5	39.45		40	41	61.81		85	86	86.76		88.6	89	90	109.5		151	152	157	158	163.6		167.1	168	169			
KI0025F	R-setting	Collar		Pkr6		#7		Pkr5		#6		Pkr4		#20		#22		Pkr3		#13?		Pkr2		#19		#21		Pkr1		END	
		0		2.5	3.5	39.45		40	41	61.81		85	86	86.76		88.6	89	90		109.5	160	161	163.6	167.1		168	169	193.7			
	S-setting	Collar		Pkr6		#7		Pkr5		#6		Pkr4		#20		#22		Pkr3		#13?		Pkr2		#19		#21		Pkr1		End	
		0		4	5	39.45		41.5	42.5	61.81		85.5	86.5	86.76		88.6	89.5	90.5		109.5	160	161	163.6	167.1		169.5	170.5	193.7			
	P-setting	Collar		Pkr4		Pkr3		#7		Pkr2		#6		#20?		#22?		#13?		#19?		#21?		Pkr1		#10		END			
		0		5	6	30		31	36.54	80		81	87.5	120.2		129.9		148.4		153.9		156.1		170		171	240	293			
KA2511A	R-setting	Collar		Pkr6		#7		Pkr5		#6		Pkr4		#20?		#22?		Pkr3		#13?		#19?		#21?		Pkr2		Pkr1		#10	
		0		5	6	36.54		63	64	87.5		91	92	120.2		129.9		138	139	148.4		153.9		156.1		170	171	230	231	240	
	S-setting	Collar	#7		Pkr7		Pkr6		#6		Pkr5		Pkr4		#20?		#22?		#13?		#19?		#21?		Pkr3		#10		Pkr2		Pkr1	
		0	36.54		51	52	54		55	87.5		91	92	109	110	120.2		129.9		148.4		153.9		156.1		216	217	240	241	242	244
	T-setting	Collar		Pkr8		#7		Pkr7		#6?		Pkr6		Pkr5		Pkr4		#20?		#22?		Pkr3		#13?		#19?		#21?		Pk	
		0		5	6	36.54		64	65	87.5		95	96	102	103	110	111	120.2		129.9		138	139	148.4		153.9		156.1		170	

Table 2-8 Virtual Packer Locations

2.15 Task 4.6.3 Tracer Test Evaluation, Phase A

Golder assisted JNC in evaluating Phase A tracer test results, in particular to determine the influence of FIZ effects on network flow and transport. This analysis pointed out dramatically lower recoveries for pathways which potentially involve FIZ. This is illustrated in Figure 2-29 and Figure 2-30.

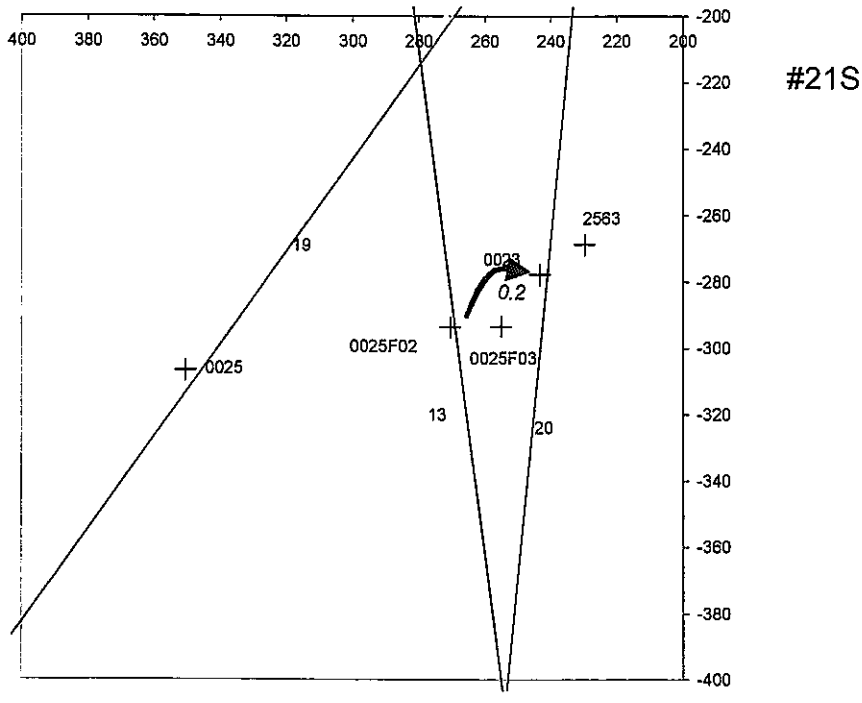

Figure 2-29 Transport Pathway in Feature 21, without FIZ Effect, Phase A Tracer Tests

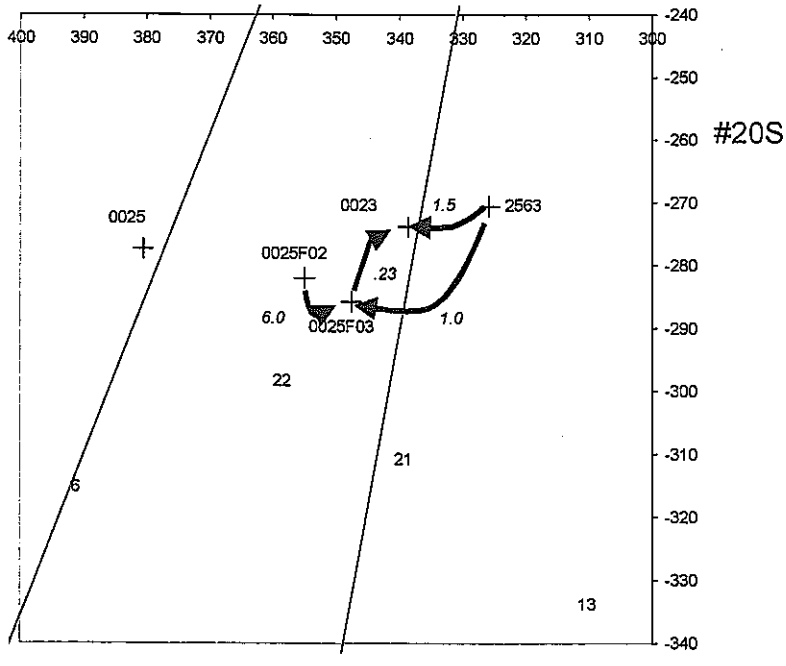

Figure 2-30 Pathways in Feature # 20, Phase A Tracer Tests

2.16 Task 4.6.4 Modeling Workshop

Golder supported JNC at two technical committee meetings regarding the results of "Phase A" tracer testing, during January and February, 2000.

2.17 Task 4.10.2 Calibration of CN Model, Phase A

Golder assisted JNC in refining the PAWorks channel network (CN) model to reflect results from Phase A tracer testing. Figure 2-31 illustrates the DFN model which provided the basis for the Phase A PAWorks modelling. The actual PAWorks model is illustrated in Figure 2-32. Phase A model calibrations were carried out against DCS Stage Pretests PT-1 and PT-2, as well as Phase A tests. Figure 2-33 illustrates the borehole array used in the Phase A interference and tracer tests. Figure 2-34 presents an example of the model calibrated to the results of Phase A hydraulic interference tests.

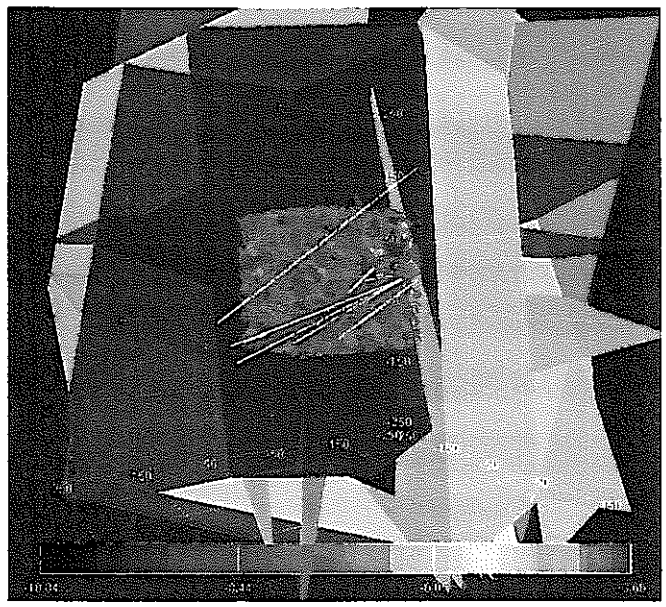

Figure 2-31 FracMan/PAWorks CN Model for Phase A

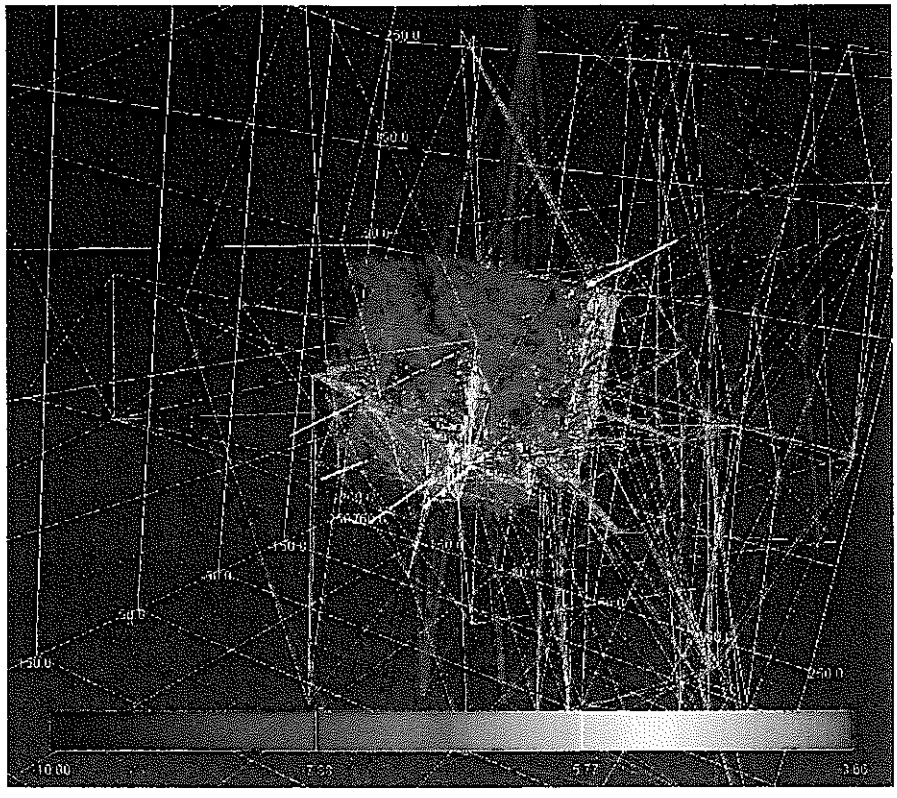

Figure 2-32 Channels in Phase A PAWorks Model

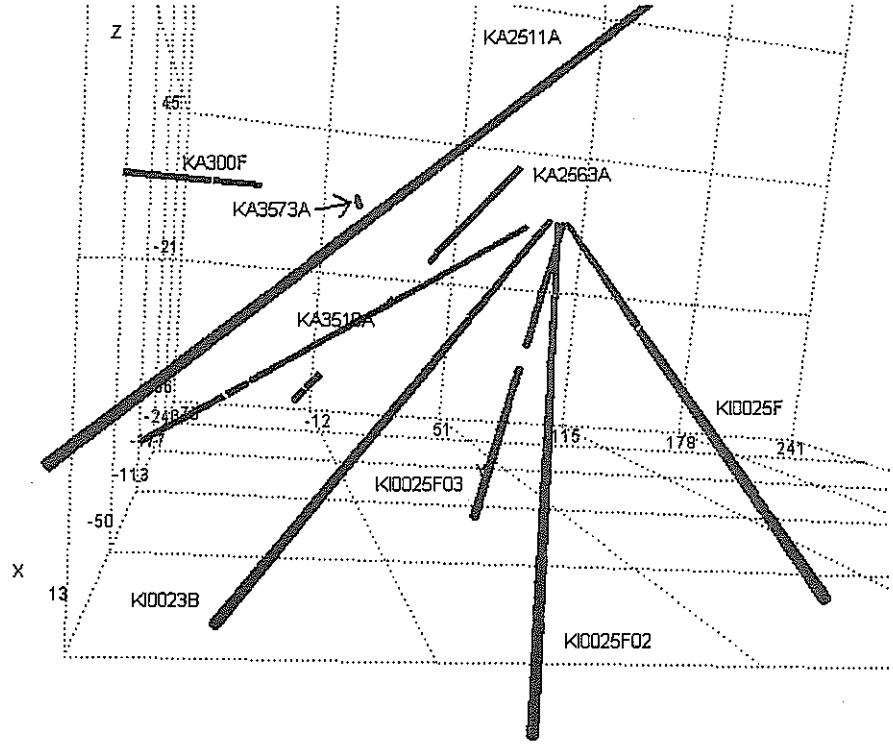

Figure 2-33 Borehole Locations for Phase A Experiments

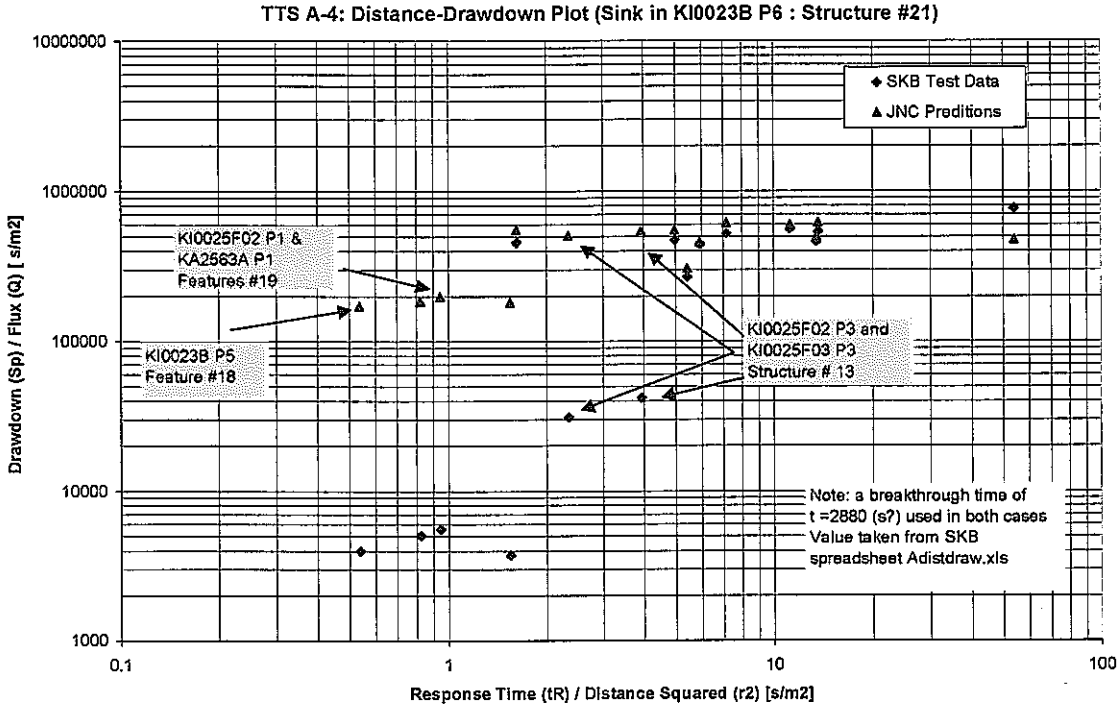

Figure 2-34 Hydraulic Interference Test Calibration for Phase A Testing

2.18 Task 4.16.5 Test Design and Structural Model Support

Golder provided extensive support for test design and structural modelling during 1999 under this task. This included:

- re-evaluation of structural models following installation of borehole KI0025F03,
- updates to structural model following pre-test and Phase-A tracer tests,
- evaluation of pre-test tracer transport and hydraulic interference results,
- evaluation of the results of Phase-A tracer tests, and
- preparation of visualization of the structural model, hydraulic, and tracer responses.

3. CONCLUSIONS

During HY-11, Golder Associates provided extensive support to JNC for participation in the TRUE-Block Scale experiment. This support has ensured that experimental configurations are designed to support JNC's project objectives, and has provided JNC with an opportunity to test a range of key hypotheses concerning flow and transport in fracture networks.

4. REFERENCES

Anderson, P., J. E. Ludvigson, and E. Wass (1999). Interference and Tracer Pre-Tests, PT-1 through PT-4. ITD 99-XX-S1. SKB, Stockholm.

Dershowitz, W., et. al. (1999). Fracman: Interactive Discrete Fracture Data Analysis Geometric Modeling, and Exploration Simulation. Golder Associates, Inc. Seattle.

Dershowitz, W., et. al. (1998). PAWorks: Pathways Analysis and Solute Transport. Golder Associates, Inc. Seattle.

Fullin, S. and L. Wei, (1997). Inpu Data for Discrete Fracture Network Modelling of the TRUE Block Scale Site. SKB Technical Note, TN-98-32b. SKB, Stockholm.

Gentzdrein, (1997, 1998). Flow Logging of Core Boreholes, True-BS rock Block. SKB Technical Note, TN-98-29b, TN-97-07b, TN-97-23b, TN-98-05b. SKB, Stockholm.

Hermanson (1999). March 1999. Structural Model Update SKB Technical Note, TN-99-XX, SKB, Stockholm.

Holton, D. (1999). Bourdag Conditions for Sub-Models at the Aspo Tree Blockscale Site. SKB, ITD 99-17. SKB, Stockholm.